Histone binding of ASF1 is required for fruiting body development, but not for genome stability in the filamentous fungus *Sordaria macrospora*

Jan Breuer[1], Tobias Busche[2,3], Jörn Kalinowski[2], Minou Nowrousian[1]

[1]Department of Molecular and Cellular Botany, Ruhr University Bochum, 44801 Bochum, Germany
[2]Center for Biotechnology, Bielefeld University, 33594 Bielefeld, Germany
[3]Medical School OWL, Bielefeld University, 33615 Bielefeld, Germany

running title:
ASF1 in fungal development

author for correspondence:
Minou Nowrousian
Department of Molecular and Cellular Botany
Ruhr University Bochum
Universitaetsstr. 150
44801 Bochum
minou.nowrousian@rub.de

Abstract

The highly conserved eukaryotic histone chaperone ASF1 is involved in the assembly and disassembly of nucleosomes during transcription, DNA replication and repair. It was the first chaperone discovered to be involved in all three of these processes. The filamentous fungus *Sordaria macrospora* is one of only two multicellular organisms where *asf1* deletions are viable, which makes it useful for *in vivo* analysis of this central part of eukaryotic chromatin structure. Deletion of *asf1* in *S. macrospora* leads to sterility, a reduction of DNA methylation, and upregulation of genes that are usually weakly expressed in the wild type. Here, we focused on the functions of the highly conserved core and the divergent C-terminal tail of ASF1, studied the effects of ASF1 on histone modifications and tested its relevance for genomic stability. By Co-IP and complementation analysis we showed that substitutions of amino acid V94 or truncations of the C-terminal tail abolish histone binding and do not complement the sterile mutant phenotype. Δasf1 is sensitive to the DNA damaging agent MMS, while complementation strains, even those with non-histone-binding variants, regain wild type-like resistance. To aid in subsequent ChIP-seq and Hi-C analyses, we generated a chromosome-resolved genome assembly of *S. macrospora*. ChIP-Seq analysis revealed a global increase of H3K27me3 in Δasf1, accompanied by a global decrease of H3K56ac. By using Hi-C we detected a tandem duplication of around 600 kb on chromosome 2 in the mutant. Crossing experiments indicated linkage between the viability of Δasf1 strains and the presence of the duplication.

Importance

Histone chaperones are proteins that are involved in nucleosome assembly and disassembly and can therefore influence all DNA-dependent processes including transcription, DNA replication and repair. ASF1 is a histone chaperone that is conserved throughout eukaryotes. In contrast to most other multicellular organisms, a deletion mutant of *asf1* in the fungus *Sordaria macrospora* is viable; however, the mutant is sterile. In this study, we could show that the histone binding ability of ASF1 is required for fertility in *S. macrospora*, whereas the function of ASF1 in maintenance of genome stability does not require histone binding. We also showed that the histone modifications H3K27me3 and H3K56ac are misregulated in the Δasf1 mutant. Furthermore, we identified a large duplication on chromosome 2 of the mutant strain that is genetically linked to the Δasf1 allele present on chromosome 6, suggesting that viability of the mutant might depend on the presence of the duplicated region.

58 **Introduction**

59 Multicellular development is a complex process that evolved independently in multiple branches of
60 eukaryotes (1). In fungi, multicellular development evolved at least twice and possibly more times, the
61 most prominent examples being the fruiting bodies of filamentous ascomycetes and basidiomycetes
62 (2). To study the genetic background of multicellular development, simple, easy to handle model
63 organisms are of particular interest. Several species of fungi have proven to be usable models for the
64 analysis of developmental processes and the generation of complex, multicellular fruiting bodies of
65 filamentous ascomycetes is an excellent example (3). *Sordaria macrospora*, a homothallic ascomycete
66 that can form its perithecia in 7 days under laboratory conditions, has been used as a model to study
67 fungal sexual development and multicellular development in general. During the formation of fruiting
68 bodies in *S. macrospora*, at least 13 different cell types are generated, many of which cannot be found
69 in vegetative mycelium (4). Sexual development and perithecia formation are accompanied by
70 transcriptional changes, and transcriptomics can be a helpful tool to identify important developmental
71 genes by reverse genetic approaches. A number of transcription factors and chromatin modifiers have
72 been identified this way and were proven to be fundamental for multicellular development (5). Among
73 them is the conserved histone chaperone ASF1 that was shown to be upregulated during sexual
74 development and is essential for this process in *S. macrospora* (6). ASF1 is involved in the assembly
75 and disassembly of nucleosomes during transcription, replication and DNA-repair and was the first
76 chaperone found to be involved in all three of these processes. It mediates nucleosome assembly and
77 disassembly in promoter regions during transcriptional activation and elongation in *Saccharomyces*
78 *cerevisiae* (7). ASF1 is also important for histone modification by interacting with enzymes that mediate
79 the corresponding modifications. For example, it has been shown to be involved in the acetylation of
80 histone H3 at lysines 9 and 56 and also to play a role in the genome-wide deacetylation of histones (8,
81 9). The methylation of histones also appears to proceed in conjunction with ASF1. In *Mus musculus*, an
82 altered distribution of H3K9me3 and H3K27me3 was shown under ASF1 deficiency. ASF1 was also
83 proven to be important for histone recycling (10). Additionally, ASF1-depleted cells were shown to
84 exhibit higher tendencies for double strand breaks, showcasing a role of ASF1 during the maintenance
85 of genomic stability (11). The function and structure of ASF1 is highly conserved in all eukaryotes. The
86 155 amino acids of the N-terminus of ASF1 form a globular core with conserved acidic patches that
87 mediate interaction with the C-terminus of histone H3. ASF1 has been shown to interact with the
88 histone H3-H4 heterodimer *in vitro* and *in vivo*. In addition to binding of H3, binding of the H4 C-
89 terminus to ASF1 also occurs. ASF1 and the H3-H4 dimer can form a heterotrimeric complex, although
90 both histones can be bound individually by ASF1 (7). The central role of ASF1 for eukaryotic chromatin
91 structure is underscored by findings in human cell lines that showed all non-DNA bound histones H3
92 and H4 are bound to ASF1 (12, 13). Therefore, researching ASF1 functions during multicellular

93 development might be fundamental for understanding the contribution of the chromatin landscape to
94 development in fungi and multicellular eukaryotes in general. Gaining insight into the functions of ASF1
95 is hindered by the fact that deletions of the respective gene are lethal in almost all higher eukaryotes.
96 Thus, research on ASF1 was mostly conducted with ASF1-depleted cell lines, *in vitro* experiments and
97 studies of the unicellular *S. cerevisiae* where an *asf1* deletion is viable (14-16). *S. macrospora* and
98 *Arabidopsis thaliana* were shown to be exceptions in this regard and deletions are viable in these
99 organisms (6, 17). Therefore, the analysis of *S. macrospora* Δasf1 strains offers the unique opportunity
100 to perform ASF1 research *in vivo* in a multicellular fungus. These strains were shown to be sterile,
101 highlighting a central role of ASF1 during sexual development. Unexpectedly, the positioning of
102 nucleosomes was not affected in *asf1* deletion strains. A significant reduction of DNA methylation was
103 observed in *S. macrospora* Δasf1, and a large number of genes that are usually weakly expressed in
104 wild type strains are upregulated in ∆asf1, indicating a role of ASF1 during gene regulation and DNA
105 methylation (18). The *S. macrospora* ASF1 has been shown to bind histones H3 and H4 (6), however, it
106 has not yet been analyzed if the histone-binding activity is actually required for fruiting body formation.
107 Therefore, in this study, we analyzed the histone binding function of ASF1 and its connection to sexual
108 development. We performed interaction studies and complementation analysis to verify the
109 importance of amino acid V94 (valine at position 94), a highly conserved histone interaction site known
110 from *in vitro* studies (7, 19). The C-terminal region of ASF1 is much less conserved than the first 155
111 amino acids and parts of it exist only in fungi (Figure 1). We generated truncated versions of this region
112 of *asf1* and used these to perform interaction studies and complementation analysis to study the
113 relevance of the divergent and functionally less well studied C-terminus of ASF1. Additionally, we
114 performed genomic stability assays based on growth under the influence of the genotoxic substance
115 methyl methansulfonate (MMS). We further focused on the role of ASF1 in histone modification and
116 chromatin structure by performing ChIP (chromatin immunoprecipitation)-seq and Hi-C (chromosome
117 conformation capture with high-throughput sequencing) experiments with the wild type and the ∆asf1
118 mutant. For improved analysis of the ChIP-seq and Hi-C data, we first generated a chromosome-level
119 genome sequence of *S. macrospora*. Participation of ASF1 in histone acetylation and deacetylation has
120 been documented in *S. cerevisiae*, and a function during histone methylation is regarded as highly
121 probable and connections to the effect on DNA-methylation and gene regulation might be possible
122 (10). Therefore, ChIP-seq was performed for H3K27me3 and H3K56ac. Furthermore, we performed Hi-
123 C experiments to compare overall chromatin structure of young, vegetative mycelium to older, sexual
124 mycelium and *asf1* deletion mutants.
125
126
127

128 ## Materials and Methods

129

130 **Strains, crosses and growth conditions**

131 All strains used in this study have been summarized in Supplemental Table 1 and were cultivated on
132 either solid or liquid cornmeal medium (BMM) or complete medium (CM) at 25 °C as previously
133 described (20, 21). To perform genetic crosses, the spore color mutant fus was used as a partner to
134 allow the identification of recombinant asci (22). Transformation of *S. macrospora* was performed as
135 previously described (21).

136

137 **Cloning procedures, oligonucleotides and plasmids**

138 Plasmids encoding ASF1 variants with amino acid substitutions for complementation and interaction
139 analysis were generated by PCR mutagenesis and yeast recombinant cloning (23). Golden Gate cloning
140 was used to assemble plasmids encoding truncated ASF1 variants (24). Oligonucleotides for the
141 generation of plasmids and integration tests have been listed in Supplemental Table 2. All plasmids
142 used in this study are listed in Supplemental Table 3.

143

144 **Histone interaction assay by Co-Immunoprecipitation (Co-Ip)**

145 Plasmids coding for eGFP-tagged ASF1 variants were co-transformed together with plasmids encoding
146 FLAG-tagged histones H3 or H4 into the *S. macrospora* wild type strain SN1693 by protoplast
147 transformation (25). The resulting strains were grown for 4 d at 27 °C in 20 ml liquid BMM medium
148 with 50 µg / ml Nourseothricin. The mycelium was harvested by filtration and frozen in liquid nitrogen
149 before being ground into powder and mixed with protein extraction buffer (26). Co-
150 Immunoprecipitation was performed according to the manufacturers' instructions using GFP-Trap®
151 Beads (Chromotek) and ANTI-FLAG® M2 Beads (Sigma Aldrich). Raw and elution fractions were used
152 for SDS-PAGE (27) before being transferred to a PVDF membrane by western blotting. Co-Ip results
153 were generated with two biological replicates each for eGFP trapping and FLAG trapping. Signals for
154 eGFP and FLAG were detected by using Mouse Anti-GFP JL-8 (Clontech), Mouse Anti-Flag (Sigma
155 Aldrich) and Goat Anti-Mouse, HRP-linked (Cell Signaling) antibodies according to the manufacturers'
156 instructions.

157

158 **Complementation of *S. macrospora* with ASF1 variants and MMS tests**

159 Plasmids for the expression of ASF1 variants were generated from wild type genomic DNA with specific
160 primers amplifying *asf1* with specific substitutions or a shortened C-terminus and cloned by Golden
161 Gate Cloning (24) or via yeast homologous recombination (28). The *asf1* deletion strain SN1983 was
162 transformed with the respective plasmids by protoplast transformation (25). Complementation strains

163 that did not gain fertility on their own were crossed against the wild type, and ascospores were isolated
164 to obtain homokaryotic strains, while fertile transformants were used to isolate ascospores directly
165 (22). Phenotypical characterization was performed by documenting the growth and fertility on BMM
166 plates with a Stemi 2000-C stereomicroscope (Zeiss). To evaluate the resistance against methyl
167 methanesulfonate (MMS) all strains were inoculated on BMM plates with 0,007 % MMS and growth
168 observed over a span of 7 d.
169
170 **Microscopic analysis**
171 For analysis of the subcellular localization of ASF1-EGFP fusion proteins, strains were grown on glass
172 slides together with strains expressing H3-MRFP fusion proteins as described (29). Light and
173 fluorescence microscopy was performed with an AxioImager microscope (Zeiss, Jena, Germany) with
174 a Photometrix Cool SnapHQ camera (Roper Scientific). EGFP fluorescence was detected with Chroma
175 (Bellows Falls, VT, USA) filter set 41017 (HQ470/40, HQ525/50, Q495lp) and mRFP fluorescence was
176 detected with set 49008 (EG560/40x, ET630/75 m, T585lp). Images were further handled by using
177 MetaMorph (Molecular Devices).
178
179 **Extraction and sequencing of genomic DNA from *S. macrospora***
180 For DNA preparation for nanopore sequencing, the wild type strain SN1693 was grown for 2 d at 27 °C
181 in 20 ml liquid CM medium (25) in petri dishes, harvested by filtration and ground in liquid nitrogen.
182 500 µg of ground mycelium was used for extraction of high molecular weight DNA with the NucleoBond
183 HMW-Kit (Macherey-Nagel, Düren, Germany) according to the manufacturer's instructions. A
184 sequencing library with wild type genomic DNA was prepared using the Nanopore DNA Ligation
185 Sequencing Kit (SQK-LSK109, Oxford Nanopore Technologies, Oxford, UK) according to the
186 manufacturer’s instructions. Sequencing was performed on an Oxford Nanopore GridION Mk1
187 sequencer using an R9.4.1 flow cell, which was prepared according to the manufacturer’s instructions.
188 Basecalling was performed using guppy v5.0.11 with the super-accurate basecalling model. A total of
189 290927 reads were obtained with an average read length of 15874 bp and an N50 of 23018 bp.
190 For DNA preparation for Illumina sequencing of the Δasf1 mutant, the Δasf1 strain SN1983 was grown
191 for 3 d at 27 °C in 20 ml liquid CM medium in petri dishes, harvested by filtration and ground in liquid
192 nitrogen. DNA preparation was performed as described previously for *Pyronema confluens* (30). Library
193 preparation and Illumina sequencing of a 300 bp insert library (150 bp paired-end sequencing) were
194 performed at Novogene (Cambridge, UK).
195
196 **Genome assembly and annotation**

197 Nanopore reads were assembled with SMARTdenovo (available at
198 https://github.com/ruanjue/smartdenovo, accessed on 2021/06/29) resulting in nine contigs with a
199 total size of 39.4 Mb. The initial assembly was subjected to four rounds of correction with Racon (31)
200 using the nanopore reads for correction, and subsequently three rounds of correction with pilon
201 (v1.24) (32) based on previously generated *S. macrospora* genomic Illumina reads (33) (NCBI SRA
202 database, accession number SRR5749461). BLAST comparisons (34) with a previously generated *S.*
203 *macrospora* genome assembly (35) showed that the smallest contig (161 kb) most likely contained
204 mitochondrial DNA. This contig was removed, and the remaining eight contigs were analyzed for
205 putative telomeric repeats (sequence TTAGGG) using a custom-made perl program. Telomeric repeats
206 were found at both ends of five contigs, and at one end each in the remaining three contigs. Of the
207 latter, one contig contained the rDNA repeats at the end without telomeric repeats. The other two
208 non-telomeric contig ends were compared to each other and found to have an overlap of 2.2 kb with
209 100 % sequence identity, making it likely that these contigs were part of the same chromosome. The
210 contigs were fused manually, and the junction was checked for continuity by mapping the nanopore
211 reads to the assembly with graphmap (36). The resulting assembly consists of 7 contigs with a total
212 size of 39.4 Mb and an N50 of 5.7 Mb. Comparison to the genome assembly of the closely related
213 ascomycete *Neurospora crassa* (FungiDB version 52) (37, 38) was performed with nucmer from the
214 MUMmer package (v4.0.0rc1) (39).
215 Genome annotation of protein-coding genes was performed with MAKER (v3.01.03) (40) based on
216 transcripts and proteins from a previous annotation of the *S. macrospora* genome (33) as well as on
217 the *N. crassa* proteins (38) from FungiDB version 52 (37). tRNAs were annotated with tRNAscan-SE
218 (v2.0.8) (41). rDNA repeats were annotated manually based on BLAST comparisons. *S. macrospora*
219 locus tags from a previous annotation (33) were mapped onto the predicted gene models based on
220 BLAST results. Approximately 1200 gene models were manually corrected in the genome browser
221 Artemis (42) based on RNA-Seq data generated previously (18, 43) (NCBI GEO accession numbers
222 GSE33668 and GSE92337) that were mapped to the assembly with Hisat2 (v2.2.1) (44).
223
224 **Western blot analysis of histone modifications and chromatin immunoprecipitation**
225 Potential targets for ChIP-seq experiments were selected based on semiquantitative western blot
226 screenings with antibodies against histone modifications previously suspected to be influenced by
227 ASF1. The wild type strain SN1693 and the Δasf1 strain SN1983 were cultivated in liquid CM medium
228 (25) for 3d and 4d, respectively, at 27 °C, harvested by filtration and washed with PPP (21). Samples
229 were frozen in liquid nitrogen and ground into a fine powder. Proteins were extracted by mixing the
230 powder with extraction buffer (50 mM Tris/HCl pH 7.5, 250 mM NaCl, 0.05 % NP-40, 0.05 % β-
231 mercaptoethanol, 0,3 % (v / v) Protease Inhibitor Cocktail Set IV (Calbiochem)) and 20 min

232 centrifugation. Protein concentrations were determined by Bradford assays (45) and equal amounts
233 were loaded and separated by SDS gelelectrophoresis and transferred to a PVDF membrane by western
234 blotting. Antibodies against target histone modifications were used to detect respective bands (Anti
235 H3K27Me3 #9733 Cell Signaling, Anti H3K9Me #ABE101 Merck Millipore, Anti H3K56Ac #61061 Active
236 Motif, Anti H3K9Ac #39038 Active Motif), detection protocols have been summarized in Supplemental
237 Table 4. Band strengths were compared by using a ChemiDoc XRS+ system (BioRad) with Image Lab 4.0
238 software (BioRad). Normalization for the total amounts of protein in the samples was based on
239 Coomassie-stained gels run in parallel. Modifications that exhibited significant differences between
240 wild type and deletion mutant were selected for ChIP-seq experiments. ChIP-samples were cultivated
241 similar to the samples for western blotting and crosslinking was performed in PPP buffer with 1%
242 formaldehyde for 15 min at room temperature, followed by a quenching time of 15 min by an excess
243 amount of glycin. After three PPP washing steps, lysis was conducted in extraction buffer (50 mM
244 Tris/HCl pH 7.5, 250 mM NaCl, 0.05 % NP-40, 0.05 % β-mercaptoethanol, 0,3 % (v/v) Protease Inhibitor
245 Cocktail Set IV (Calbiochem)) for 15 min on ice by frequent vortexing. After centrifugation, chromatin
246 solution was obtained and mixed with MNase Buffer (18) and proteinase inhibitors. Chromatin
247 digestion was conducted by incubation with 200 U/ml MNase (Thermo Fisher Scientific) for 105 min at
248 37 °C under constant shaking and stopped by adding EDTA to a concentration of 20 mM. Aliquots were
249 removed as input samples, and immunoprecipitation performed over night at 4 °C on a spinning wheel
250 by adding 10 µl of the respective antibody (Anti H3K27Me3 #9733 Cell Signaling, Anti H3 #2650 Cell
251 Signaling, Anti H3K56Ac #61061 Active Motif). Afterwards, 4h of incubation on Protein-A agarose
252 beads (Santa Cruz) were followed by 2 washing steps in low salt and 2 washing steps in high salt buffer.
253 Each washing step was performed for 5 min at 4 °C on a spinning wheel and followed by 2 min of
254 centrifugation at 2500 rpm to separate the beads from the buffer (46). Chromatin was washed off the
255 beads by 2 h of incubation in TE buffer with 1 % SDS at 65 °C and de-crosslinked over night at 65 °C
256 after adding 2 mg/ml Proteinase K (Genaxxon bioscience). Standard phenol/chloroform extraction was
257 performed to isolate DNA from the ChIP and input samples. Two biological replicates each were
258 created for H3, H3K27me3 and H3K56ac. Library generation and Illumina sequencing (150 bp paired-
259 end) of ChIP and input samples were performed by Novogene (Cambridge, UK). The detailed ChIP-seq
260 protocol can be found in Supplemental Text 1.
261
262 **ChIP-seq peak detection**
263 20 million paired-end reads per sample were obtained, trimmed with fastp 0.23.2 (47) and mapped to
264 the reference genome of *S. macrospora* SN1693 by using BWA-MEM 0.7.17 with default parameters
265 (48). Input corrected peak detection was performed for the duplicated samples of H3, which were
266 subsequently used together with the native input samples as control for H3K27me3 and H3K56ac by

267 using MACS2 callpeak 2.2.7.1 in paired end mode with a 0.01 minimum FDR (false discovery rate) cutoff
268 for broad regions and an effective genome size of 39 Mb (49, 50). Differential peak analysis was
269 conducted by discarding overlapping peaks in wildtype and Δasf1 using BEDTools 2.30.0 with a
270 minimum overlap of 10 % (51). Peaks were annotated to the reference genome using HOMER
271 annotatePeaks 4.9.1 (52).
272
273 **Hi-C sample preparation**
274 Young wild type samples of SN1693 where cultivated for 2 d at 27 °C in liquid CM medium (25). Samples
275 for the older wild type where grown for 5 d and Δasf1 SN1983 for 3 d under the same conditions.
276 Mycelium was harvested by filtration, washed with PPP (21) and frozen in liquid nitrogen. The Omni-C
277 library was prepared using the Dovetail® Omni-C® Kit according to the manufacturer's protocol with
278 additional changes to enable the use on *S. macrospora*. Briefly, the chromatin was fixed with 1 %
279 formaldehyde for 10 min at room temperature on a spinning wheel and quenched by bringing the
280 solution up to 200 mM glycine. The cross-linked chromatin was then digested in situ with DNase I
281 according to the manufacturer's instructions. Following digestion, the cells were lysed in 1 % SDS to
282 extract the chromatin fragments and the chromatin fragments were bound to Chromatin Capture
283 Beads. Next, the chromatin ends were repaired and ligated to a biotinylated bridge adapter followed
284 by proximity ligation of adapter-containing ends by using the reagents supplied by the Dovetail® Omni-
285 C® Kit. After proximity ligation, the crosslinks were reversed at 68 °C in Dovetail® Crosslink Reversal
286 Buffer and 1 µg / µl Proteinase K overnight. The DNA was purified with SPRIselect™ Beads (Beckmann
287 Coulter) and 150 ng were converted into a sequencing library using Illumina-compatible adaptors by
288 using the Dovetail® Library Module for Illumina®. Biotin-containing fragments were isolated using
289 streptavidin beads prior to PCR amplification. Illumina sequencing (150 bp paired-end) was performed
290 by Novogene (Cambridge, UK).
291
292 **Generation of Hi-C maps**
293 Hi-C maps were created by following the Dovetail® Omni-C® Pipeline with adjustments for the genome
294 of *S. macrospora*. 50 million paired end reads were obtained, trimmed with fastp 0.23.2 (47) and
295 mapped to the reference genome of *S. macrospora* SN1693 by using BWA-MEM 0.7.17 with default
296 parameters (48). Valid ligation events were recorded by using pairtools 1.02 (53) parse with a min-map
297 quality of 40 and a max-inter-align-gap of 30 before being sorted by pairtools sort. PCR duplicates were
298 removed by using pairtools dedup and the pairs file was generated by pairtools split. The hic matrix
299 was generated by using juicertools 1.6.2 (54) with standard parameters.
300
301 **Data availability**

302 Nanopore reads and the chromosome-resolved genome sequence for the *S. macrospora* wild type
303 strain SN1693 were deposited in the NCBI databases under BioProject ID PRJNA744349
304 (http://www.ncbi.nlm.nih.gov/bioproject/744349, SRA accession number SRR15901728 for the
305 nanopore reads, DDBJ/ENA/GenBank accession numbers CP083903-CP083909 for the seven
306 chromosomes). ChIP-seq and Hi-C data generated in this study were submitted to the NCBI GEO
307 database as a superseries under accession number GSE216634
308 (https://www.ncbi.nlm.nih.gov/geo/query/acc.cgi?acc=GSE216634, accession numbers GSE216629
309 and GSE228529 for ChIP-seq data and GSE216632 for Hi-C data). Illumina reads from the Δasf1 strain
310 were deposited in the NCBI SRA database under BioProject ID PRJNA922040
311 (https://www.ncbi.nlm.nih.gov/sra/PRJNA922040).
312
313
314 **Results**
315
316 **A chromosome-level genome assembly of *S. macrospora***
317 The nuclear genome of *S. macrospora* was previously shown by pulsed-field gel electrophoresis to
318 consist of seven chromosomes (21). Prior to our study, three genome assemblies of *S. macrospora*
319 have been generated with increasing continuity (33, 35, 55); however, even the latest genome
320 assembly still consists of 584 scaffolds (33) and would therefore be unsuited for analyses at
321 chromosome level. Therefore, to aid in the planned Hi-C and ChIP-seq analyses, we generated a
322 chromosome-level genome assembly of *S. macrospora* based on nanopore sequence reads. The new
323 assembly (*S. macrospora* genome version 04) consists of seven gapless contigs with a total size of 39.4
324 Mb (Figure S1) which is similar in size to previous assemblies and to estimates by pulsed-field gel
325 electrophoresis of 39.5 Mb (21, 33, 35, 55). Six of the seven contigs have telomeric repeats at both
326 ends, whereas one contig has telomeric repeats at one end and 10 copies of the ribosomal RNA (rRNA)
327 genes at the other end with the repetitive nature of the rRNA genes most likely preventing assembly
328 of telomeric repeats at that end. This indicates that the seven contigs represent the seven
329 chromosomes of *S. macrospora*. A comparison with the genome assembly of the closely related
330 ascomycete *Neurospora crassa* showed a high degree of synteny for the seven chromosomes of each
331 species, consistent with previous analyses of smaller genomic regions of the two fungi (35, 56) (Figure
332 S1). Thus, a chromosome-level assembly for *S. macrospora* is now available and can be used for
333 analyses at chromosome level.
334
335 ***S. macrospora* ASF1 depends on V94 and large parts of the C-terminus to accomplish histone binding**

336 The function and structure of ASF1 is highly conserved in all eukaryotes and it has been described as a
337 central histone chaperone that binds the histones H3 and H4 as a dimer and individually. The first 155
338 amino acids form a globular core in which acidic patches allow for the interaction with both histones
339 (7). Especially the area surrounding position V94 has been shown to be essential for ASF1-histone
340 binding in yeast (19). However, little is known about the functions of the C-terminal tail. This region is
341 much more divergent than the globular core and parts of it exist only in fungi (Figure 1). To analyze if
342 V94 is required for histone binding of *S. macrospora* ASF1, we performed co-immunoprecipitation
343 experiments with an ASF1 variant that includes a V94R substitution and a variant with a D37A
344 substitution. The latter is a mutation of an interaction site with the histone chaperone HIRA that was
345 identified in *S. pombe* (57). In addition, ASF1 variants with truncations after positions 152, 185 and 210
346 were generated to gain insight into possible involvement of the C-terminal region in the process of
347 histone binding. In GFP- and FLAG-trap experiments, the V94R variant proved to be incapable of pulling
348 down the histones H3 and H4, while the D37A variant performed like the wild type ASF1 (Figure 2).
349 Thus, the conserved V94 is required for histone interactions in *S. macrospora*, whereas the putative
350 HIRA interaction site D37 is not. Truncated ASF1 variants were also unable to bind H3 and H4 when
351 the truncations occurred after positions 152 or 185. Truncation after position 210 had no detectable
352 effect and did not impair the capability to pull down the histones (Figure 3).
353
354 **The histone binding function of ASF1 is essential for sexual development**
355 Deletions of *asf1* are usually lethal in higher eukaryotes, making research into its involvement in
356 multicellular development very challenging. *S. macrospora* and *A. thaliana* are the only known
357 exceptions that have been discovered so far (17, 18). The qualities of *S. macrospora* as an easy to
358 handle and fast propagating model organism with the ability to form complex, multicellular structures
359 during sexual development make it an exceptional tool for *asf1 in vivo* research. We used the *asf1*
360 variants described above carrying substitutions in the histone binding site V94, the putative HIRA
361 interaction site D37 and variants with truncated C-terminal regions for complementation analysis in a
362 previously constructed *asf1* deletion strain (6). By correlating the ability of these variants for rescuing
363 the phenotype of the deletion mutant with information about their ability to bind histones, more
364 insights into the role of ASF1-histone interaction during multicellular development can be gained. The
365 *asf1* deletion mutant was transformed with plasmids coding for the respective variants, and
366 homokaryotic strains were obtained by the isolation of ascospores from self-fertile perithecia or from
367 genetic crosses. PCR screenings confirmed the integration of *asf1* variants in the resulting
368 transformants (Figure S4). The phenotype of the resulting strains was documented after growth for a
369 week on BMM medium. *S. macrospora* Δasf1 is sterile and mostly consists only of vegetative mycelium,
370 but is sometimes able to generate small protoperithecia. Introducing the wild type *asf1* gene back into

371 the deletion mutant led to a complete reversal of the deletion phenotype and yielded strains
372 indistinguishable from the wild type, gaining full fertility. Strains expressing the D37A variant also
373 regained fertility and were able to form perithecia, but showed slight aberrations. A tendency to grow
374 giant protoperithecia and a distinct brown color of the mycelium and ascospores was observed. A
375 reintroduction of an ASF1 variant with a V94R substitution did not complement the deletion mutant
376 and the resulting strains exhibited the same phenotype as Δasf1 strains (Figure 4, Table 1). Since ASF1
377 V94R does not complement the sterile phenotype of deletion mutants and is unable to bind histones,
378 a connection between histone binding and sexual development seems likely. ASF1 D37A proved to
379 have no disruption in histone binding and regained fertility, but the substitution in a putative HIRA-
380 binding site still had impact on the life cycle of *S. macrospora*. However, histone binding capability was
381 enough to reach fertility. Truncations of ASF1 at positions 152 and 185 led to strains that resembled
382 the deletion mutant, but a truncation at position 210 still allowed for full complementation (Figure 4,
383 Table 1). Thus, although the C-terminal tail of ASF1 is less conserved, parts of it are essential for histone
384 binding and sexual development. Leaving only the core intact, or shortening the protein to 185 amino
385 acids seems to have the same effect on both processes as a full deletion. A truncation after position
386 210 removes the part of ASF1 that is only present in fungi and does not affect its overall functionality.
387 To rule out the possibility of mislocalization as a cause for the inability to complement the deletion
388 mutant, the eGFP-tagged variants were tracked by fluorescence microscopy. All of them co-localized
389 with an mRFP-tagged H3 in the nucleus (Figure S5), similar to what was previously shown for wild type
390 ASF1 (6).
391
392 **ASF1 can contribute to DNA damage protection even without histone binding capabilities**
393 Even after confirming the correct localization of tested ASF1 variants, a possible complete loss of
394 function of the protein, i.e. not specifically related to histone binding, could not be completely ruled
395 out. Thus, we looked for a way to confirm functionality of the variants aside from histone binding *in*
396 *vivo*. The complex network of ASF1 regarding chromatin modification is still poorly understood and
397 direct functions beyond nucleosome assembly are not widely known. It was previously show in *S.*
398 *cerevisiae* that ASF1 is involved in DNA damage protection, since Δasf1 mutants are unable to grow on
399 the DNA damage-inducing agent MMS (58). However, in *S. cerevisiae* C-terminal truncations had no
400 impact on DNA damage protection abilities of ASF1 (59, 60). Therefore, we tested *S. macrospora* Δasf1
401 and the strains expressing the variants for their reaction to the DNA damaging agent MMS, which
402 causes DNA single- and double strand breaks. At a concentration of 0.007 % MMS (v/v), the wild type
403 was able to grow normally on BMM medium, while the mutant did not grow at all (Figure 5).
404 Complementation strains expressing ASF1 variants D37A and 210T showed wild type-like resistance.
405 Although the V94R, 152T and 185T variants of ASF1 are indistinguishable from the deletion strain

406 under normal conditions, an increased resistance against MMS compared to the ∆asf1 strain was
407 clearly visible (Figure 5). The difference between *S. macrospora* strains expressing these ASF1 variants
408 and the deletion mutant suggests that an uncharacterized function of ASF1 in DNA damage protection
409 exists and these variants are functional in this regard even though they are not able to bind histones.
410 Thus, the data suggest that the role of ASF1 in DNA damage protection does not depend on histone
411 interaction.
412
413 **Deletion of *asf1* changes global histone modification levels in *S. macrospora***
414 The functions of ASF1 as a central histone chaperone and its multiple interaction partners during
415 chromatin modification suggest a participation in processes like histone modification. Indeed, ASF1
416 has been shown to be involved in the acetylation of H3 on the lysines 9 and 56 in *S. cerevisiae* (9) and
417 changes in the disposition of H3K27me3 and H3K9me3 have been observed in *M. musculus* cells during
418 ASF1 depletion conditions (10). To gain insight into the role of ASF1 in histone modification, we
419 performed semi-quantitative western blot screens with protein extracts from *S. macrospora* wild type
420 and Δasf1 for histone modifications H3K27me3, H3K9me, H3K56ac, and H3K9ac. The comparison of
421 the band strength after incubation with antibodies specific for these modifications indicate significant
422 changes in global histone modification levels for H3K27me3 and H3K56ac in the ∆asf1 mutant (Figure
423 6 A-B). H3K27me3 levels were upregulated in the deletion mutant, while a depletion of H3K56Ac could
424 be observed. Thus, we chose these histone modifications as candidates for ChIP-Seq experiments to
425 verify the results of the screening and to gain information about the local distribution of both histone
426 marks. Establishing this method for older mycelium of *S. macrospora* presented challenges regarding
427 the crosslinking and shearing process, as crosslinking agents appeared to create an agglomeration of
428 inaccessible cells. A combination of high input amounts, soft lysis conditions and DNase based
429 shearing, allowed us to conduct reproducible ChIP-seq experiments on older *S. macrospora* samples
430 for the first time (Supplemental Text 1). Matching the results of the Western blot analysis, ChIP-seq
431 revealed that the amount of H3K27me3 was significantly increased on a global level in the deletion
432 mutant (Figure 6 C). Local distribution regarding functional regions like transcription start sides and
433 gene bodies did not undergo significant changes, albeit looking at the peaks which only exist in wild
434 type or ∆asf1, a slight shift from intergenic regions into exon regions occurred in the *asf1* deletion
435 mutant (Figure 6 E). H3K56ac levels appeared to be reduced in the deletion mutant, although this
436 euchromatin mark was still present. Focusing on the unique H3K56ac positions in either ∆asf1 or the
437 wild type revealed that almost no nucleosomes were uniquely marked in *S. macrospora* Δasf1 whereas
438 the wild type exhibits a far higher abundance of specific H3K56ac positions (Figure 6 D). The specific
439 H3K56ac positions in the mutant seemed to be more prevalent in exons, compared to the wild type
440 (Figure 6 F).

441

442 **Hi-C reveals a 600 kb duplication in *asf1* deletion mutants that might be linked to their survival**

443 To study the effect of *asf1* and sexual development on overall chromatin structure, we performed Hi-
444 C experiments to map the abundance of DNA-DNA interactions in mycelium at two different
445 developmental stages of the wild type and in mycelium of Δasf1. Samples for the young wild type were
446 grown for 2 d, thus most of the mycelium consisted of vegetative tissue and sexual development was
447 in its early stages. Samples for older mycelium were grown for 5 d, at this stage fully melanized
448 protoperithecia and some early perithecia can be expected. The deletion mutant was cultivated for 3
449 d (since it is growing somewhat slower than the wild type), but is blocked in its sexual development at
450 the stage of very young protoperithecia. The chromatin of the samples was fixed with formaldehyde
451 and treated with DNase to obtain crosslinked pairs of DNA that are in close proximity at that time. Ends
452 were filled with biotin and re-ligation was performed under high dilution conditions, so ligation events
453 of crosslinked strands are more likely. A streptavidin pulldown was used to generate samples
454 containing interacting DNA fragments of a sample at the given time. By using Dovetail® Dual index
455 primers, Illumina® libraries of around 50 ng were obtained and used for high throughput paired end
456 sequencing. 50 million paired end reads per sample were used for the generation of Hi-C maps. All
457 recorded interaction events were plotted against their position on the *S. macrospora* genome, each
458 one represented by a red dot. The intensity of red dots at a specific area indicates more recorded DNA-
459 DNA interactions in the sample at the tested point in time. The characteristic diagonal line is an
460 indicator of the high interaction frequency of genomic regions that are always in close proximity to
461 each other, because of their vicinity on the DNA strand itself (Figure 7). While the resolution of the
462 generated HI-C maps was too low to make out specific compartments of the young and old wild type,
463 a significant reduction of the general resolution in the sexual mycelium might hint at the development
464 of multiple cell types with different chromatin conformations. During sexual development *S.*
465 *macrospora* generates multiple different cell types (4), therefore it seems likely that different cell types
466 are characterized by different chromatin conformations. The presence of more than one chromatin
467 conformation in a sample could lead to a loss of signal for mappable DNA-DNA interactions at a specific
468 point. The Hi-C map of the deletion mutant appeared to show a strong increase of DNA-DNA
469 interactions of a specific region of 600 kb on chromosome 2 with all other genomic regions (enhanced
470 horizontal and vertical bars in Figure 7). However, such an explanation is biologically unlikely, and a
471 more likely explanation would be that this genomic region in the ∆asf1 mutant differs from the wild
472 type genome that was used as a reference for mapping. In this case, this strong increase hinted at a
473 duplication of this region in Δasf1, which would result in twice the number of reads, which then all
474 mapped to the single copy of the wild type genome that was used as a reference for the generation of
475 the Hi-C map. This would also lead to twice the number of (spurious) interactions with other regions

476 of the genome, which would appear as the observed enhanced horizontal and vertical bars in the Hi-C
477 contact map. We detected read patterns in the Hi-C data that match the internal border of a putative
478 tandem duplication of the area of interest. To test this, we sequenced the genome of the ∆asf1 mutant
479 by Illumina sequencing. Sequencing reads were mapped to the wild type reference genome, which
480 proved the existence of the duplication in the deletion mutant (Figure 8 A). The detected duplication
481 consists of two compartments, with the middle region of the area of interest not duplicated, hinting
482 at a loss event or two independent duplication events. PCR tests with primers amplifying the newly
483 created internal junctions of the duplicated area (Figure 8 B) revealed the existence of the duplication
484 in all used ∆asf1 strains even those that resulted from backcrosses against the wild type. Since the *asf1*
485 gene is located on chromosome 6, whereas the duplication is present on chromosome 2, they should
486 segregate independently resulting in approximately 50 % of ∆asf1 strains with and 50 % without the
487 duplication in a cross with a wild type strain. Therefore, we suspected that the viability of the *asf1*
488 deletion might depend on the presence of the duplication. Crossing experiments were performed to
489 analyze the correlation between viable Δasf1 strains and the duplication. The crosses with the spore
490 color mutant fus, which carries the wild type *asf1* allele, resulted 69 strains with an *asf1* wild type
491 allele, of which 21 contained the duplication, matching expectations for free recombination. The 37
492 ∆asf1 mutant strains all possessed the duplication, suggesting that the viability of ∆asf1 strains is
493 indeed linked to the occurrence of the duplication on chromosome 2 (Table 2). During screenings for
494 duplication-free Δasf1 strains, we also screened strains carrying the *asf1* variants we used in the
495 complementation analysis and detected the absence of the duplication in an ASF1-V94R strain
496 (Supplemental Table 5). This variant is unable to bind histones and does not complement the
497 developmental phenotype of *asf1* deletions, but is able to contribute to the resistance against
498 genotoxic stress. This suggests that the presence of an ASF1 protein even without histone binding
499 ability is sufficient to overcome the potential lethality of the complete absence of ASF1, whereas the
500 complementation studies described above show that ASF1 without histone binding ability is not
501 sufficient for fruiting body development.
502
503
504 **Discussion**
505
506 ***S. macrospora* ASF1 needs an intact C-terminal region to perform histone binding, an essential**
507 **function for sexual development**
508 Next to *A. thaliana* (17), *S. macropspora* is one of only two known multicellular organisms that survive
509 a full deletion of *asf1* (even though this might be contingent on the presence of the duplication on
510 chromosome 2 as described above), making it a valuable model for ASF1 *in vivo* research, especially

511 when its fast vegetative growth and sexual cycle are taken in account. Therefore, we have the unique
512 opportunity to study the importance of *asf1* for multicellular development. *asf1* deletion strains have
513 been shown to exhibit a slowed vegetative growth rate, and sexual development is blocked at the
514 stage of young protoperithecia (6).
515 The ability to interact with histones can be regarded as the central requirement of a histone chaperone
516 to perform its functions. ASF1 is known to interact with the histones H3 and H4 and deposits them
517 during nucleosome assembly during transcription, replication and DNA-repair. The general interaction
518 mode of ASF1 with H3 and H4 has been analyzed by *in vitro* experiments with *S. cerevisiae* proteins.
519 The central acidic patch in the core of ASF1 and especially the amino acid V94 are essential in this
520 regard (7). Since the first 155 amino acids of ASF1 are highly conserved in all eukaryotes, similar
521 functions can be assumed. In fact, our co-immunoprecipitation experiments showed a clear
522 dependency of *S. macrospora* ASF1 on V94 to establish interactions with H3 and H4. However, the C-
523 terminal region of ASF1 is quite divergent, with some parts existing only in fungi, and information about
524 the functional relevance of this region is sparse. Although experiments in *S. cerevisiae* showed a
525 contribution of the C-terminal region of ASF1 to histone interaction and gene silencing, the specific
526 interaction mode still remains elusive (59). Since the unicellular nature of yeasts does not allow for the
527 analysis of multicellular developmental processes and the specific region of ASF1 is quite divergent,
528 experiments in multicellular eukaryotes like *S. macrospora* might shed more light on the functions of
529 this part of ASF1. Co-immunoprecipitation showed that despite of this region's divergent nature it is
530 essential for establishing a connection between ASF1 and H3-H4 up until amino acid 210. Thus, a
531 function of the C-terminal tail during this interaction is highly likely. The acidic nature of the C-terminal
532 tail might contribute to facilitating the connection between ASF1 and the histones. A physical
533 interaction between the C-terminal region and H3-H4 has not yet been detected, but might be difficult
534 to prove with structural analysis, because of the usually unfolded C-terminus (58). ASF1 is known to
535 bind histones H3 and H4, but prior to this study, it was not clear if histone binding is required for sexual
536 development. We therefore analyzed different ASF1 variants for their ability to bind histones as well
537 as their ability to support fruiting body formation. Since all ASF1 variants that did not co-
538 immunoprecipitate the histones H3 and H4 were unable to restore the deletion phenotype, the histone
539 binding function of ASF1 appears to be fundamental for sexual and therefore complex multicellular
540 development. Complementation experiments with ASF1 variants that were shown to be able to bind
541 histones led to fully fertile strains, underscoring the importance of this function for normal
542 development. With the exception of ASF1 D37A, these variants generated *S. macrospora* strains that
543 resembled the wild type. D37A strains exhibited a light brown coloration of the mycelium and had a
544 tendency to generate giant protoperithecia. Since D37 is the putative interaction site of ASF1 with the

545 histone chaperone complex HIRA (19), one might speculate about an involvement of HIRA during
546 melanin biosynthesis and sexual development.
547
548 **Histone binding is not essential for the function of ASF1 during DNA-damage repair**
549 A role of ASF1 during DNA-damage repair without usage of its histone chaperone activity has often
550 been suspected and indeed, in recent studies with human ASF1A, a connection to double strand repair
551 mechanisms independent of histone binding has been discovered (61). In *S. macrospora*, strains
552 expressing ASF1 variants defective in histone binding were able to survive genotoxic stress, whereas
553 Δasf1 proved to be highly sensitive. It can therefore be concluded that the constructed ASF1 variants
554 are all functional in DNA damage repair and that the observed defects in fruiting body development
555 are specifically related to the ability to perform canonical histone chaperone functions. One hypothesis
556 might be that ASF1 is not only a histone chaperone, but also functions as a chromatin modifier hub
557 that regulates and supports the activity of other chromatin-modifying proteins. Regarding the
558 involvement in DNA damage repair, multiple interaction partner candidates are conceivable. A histone-
559 independent interaction with RIF1 has already been demonstrated in human cell lines and contributes
560 to determining the choice of the appropriate double strand break repair mechanism (61). Another
561 candidate involved in DNA damage protection and possibly activated by ASF1 is the histone
562 acetyltransferase RTT109. RTT109 is responsible for H3K9 and K56 acetylation, modifications that are
563 known to be important for DNA damage resistance (62). Interaction between ASF1 and RTT109 has
564 been characterized for *S. cerevisiae* (9) and an activating effect on the histone acetyltransferase was
565 shown, although the exact mechanism remains elusive (63). A defect in acetylation of H3 in *asf1*
566 deletion mutants has been also demonstrated in our ChIP-Seq experiments, therefore a connection
567 between the increased sensitivity of *S. macrospora* Δasf1 to DNA damage and lowered activity of
568 RTT109 seems possible. Another ASF1-mediated factor for DNA stability is known in *S. cerevisiae* as
569 the checkpoint kinase RAD53 and is involved in DNA-double strand break repair mechanisms. RAD53
570 needs to be inactivated and bound to ASF1 after repair has been completed, and lack of ASF1 could
571 lead to an overabundance of active RAD53 and subsequent disturbances in the cell cycle and further
572 damage repairs (64). All in all, ASF1 seems to play a crucial role during multiple DNA-damage protection
573 and repair pathways, not all of them relying on ASF1-H3/H4 interactions.
574
575 **ASF1 is involved in the histone modification landscape of *S. macrospora***
576 The histones are targets of various posttranslational modifications. The best known are acetylation,
577 methylation, phosphorylation, sumoylation, and ubiquitination. These modifications vary throughout
578 the genome and shape the histone code, which in turn influences access to the DNA for transcription
579 and the recruiting of transcription factors. The histone landscape of a cell is a significant determinant

580 of the transcriptome (65). ASF1 as a central eukaryotic histone chaperone has been reported to affect
581 multiple histone modifications, such as acetylation of H3K56 (9) and methylation of H3K27 (10). These
582 modifications undergo significant changes after deletion of *asf1* in *S. macrospora*. For H3K27me3, a
583 well-known heterochromatin modification (66), *asf1* deletion mutants showed almost three times as
584 many unique H3K27 trimethylations as the wild type. The increase in unique H3K27me3 positions did
585 not seem to be very site specific, as the relative distribution was comparable in the mutant and the
586 wild type. In general, we did not observe a significant change of H3K27me3 in specific functional
587 regions, like transcriptional start sites or gene bodies. The increase of H3K27me3 in *asf1* deletion
588 strains could either be a direct consequence of lack of activation of a corresponding methyltransferase,
589 or a compensatory reaction to the absence of ASF1. ASF1 is known to be involved in the recycling of
590 histones during DNA replication (7). H3K27me3 is an inheritable histone modification that can persist
591 during replication and the *de novo* integration of histones by ASF1 and CAF1 in parental cells was
592 shown to heavily dilute the inheritance of this mark in nascent chromatin in *A. thaliana* (67). Therefore,
593 a reduction in *de novo* nucleosome assembly through the deletion of a major histone chaperone like
594 ASF1 could reduce general recycling of histones and cause the already established H3K27me3 to persist
595 and accumulate. Especially genomic regions that do not carry H3K27me3 all the time under wild type
596 conditions would show a visible increase under such circumstances, matching our observations of
597 significantly more uniquely marked positions in the deletion mutant. The blocking of nucleosome
598 recycling and the resulting more permanent marking of histones with H3K27me3 might be an
599 explanation for the severe developmental phenotype of *S. macrospora* Δasf1. Genome wide
600 redistribution of H3K27me3 has been linked to defects in sexual development in *N. crassa*, a close
601 relative of *S. macrospora* (68), so the persistence of this mark in regions where it would exist only
602 temporarily in the wild type might cause similar effects. However, the changes in H3K27me3
603 distribution could also be a reaction to the reduced DNA methylation observed in ∆asf1 (18). In
604 addition to a global reduction of DNA methylation, the deletion of the *S. macrospora asf1* leads to an
605 increase in transcription of many usually weakly expressed genes (18). DNA methylation and
606 H3K27me3 are mostly considered to be marks of transcriptionally silenced regions, but are often
607 regarded as antagonistic to each other (69). Thus, the observed global increase in H3K27me3 in a
608 deletion mutant that also shows a decrease in DNA methylation could be the result of a compensation
609 mechanism for the loss of a transcriptional silencing mechanism. The rising transcription levels
610 resulting from the DNA methylation loss might be kept at least in an acceptable range by using other
611 transcriptional silencers, such as H3K27me3 to keep the deletion mutant alive. This effect might
612 therefore be one of the reasons why *S. macrospora* survives full *asf1* deletion and other multicellular
613 organisms do not.

614 Histone acetylations on the other hand are known as euchromatin markers, their negative charge can
615 lower the overall positive charge of histones and weaken their binding to the DNA. This can facilitate
616 a more relaxed and open chromatin state that can be accessed by RNA polymerases (70). The higher
617 transcription rates of usually weakly expressed genes after the deletion of *asf1* in *S. macrospora* might
618 suggest that euchromatin marks could be in higher abundance in such a strain. For H3K56ac, our ChIP-
619 Seq results showed that at least for this mark, the opposite is the case and the mutant exhibits less
620 H3K56 acetylation on a global scale. As with the heterochromatin mark H3K27me3, we were not able
621 to detect specific patterns of acetylation loss, the overall abundance of the mark appeared to be
622 reduced. This coincides with the higher sensitivity of Δasf1 strains to genotoxic stress. H3K56ac has
623 been described to be of high importance for DNA damage repair (71). Strikingly, we still detected
624 H3K56ac during western blot screenings, as well as ChIP-Seq experiments, while it has been reported
625 that the presence of ASF1 is required to generate this mark in *S. cerevisiae* (72). A significant reduction
626 of H3K56ac levels in *S. macrospora* Δasf1, however, might be an explanation for the severe sensitivity
627 to genotoxic stress of those strains. H3K56ac is known as an important factor for genomic stability and
628 resistance against replication fork damage, as studies in yeast have shown (73). Since this mark is
629 generated by the histone acetyltransferase RTT109, which is activated by ASF1 (63), it can be
630 speculated that the lower abundance of H3K56ac and the genomic instability are resulting from a lack
631 of ASF1-RTT109 interaction. Additionally, the presence of H3K56ac in *S. macrospora* Δasf1, even
632 though ASF1 was expected to be required for the generation of this mark, hints at either an unknown
633 second activation pathway for RTT109, or an undiscovered way to establish H3K56ac in multicellular
634 ascomycetes. Taken together with the detected increased levels of the heterochromatin mark
635 H3K27me3, lower euchromatic H3K56ac levels would suggest an all-around lower general
636 transcriptional activity of *S. macrospora asf1* deletion mutants. Since the opposite has been
637 documented (18), it can be hypothesized that the contribution of ASF1 to regulating the transcriptome
638 is either not mainly mediated by histone modifications, or is even more complex than previously
639 assumed.
640
641 **Hi-C analysis reveals a 600 kb duplication in *S. macrospora* Δasf1 which might be linked to its viability**
642 Methods such as Hi-C allow the analysis of the three-dimensional organization of the chromatin and
643 its effects on the transcriptome and gene regulation. The relationship between chromatin structure
644 and gene regulation seems to be quite complex and possibly both processes can regulate each other
645 (74). In this study, we created DNA-DNA interaction maps of the young, mostly vegetative state of *S.*
646 *macrospora* and compared it to older mycelium, which has progressed in the cycle of sexual
647 development and an *asf1* deletion mutant with the aim of identifying differences in the chromatin
648 state of those samples. The major challenge was the application of a method that has been fine tuned

649 for single cell assays and fungal protoplasts to older, more mature fungal mycelium. The resulting map
650 of the young wild type showed some areas of the chromatin that suggested higher condensation than
651 other areas, but in general the resolution was not high enough to confidently identify specific
652 interaction compartments. An even lower resolution was visible for the Hi-C map of the older, sexual
653 sample. But the lower DNA-DNA interaction in this case could be a sign of multiple different chromatin
654 states. Entering sexual development, *S. macrospora* begins generating more specialized cell types, at
655 least 13 different cell types have been identified during fruiting body formation of this fungus (4).
656 Different functions of cells require different transcriptomic processes, which can depend on specific
657 changes of the three-dimensional chromatin state. Higher differentiation of cells in a sample and
658 therefore more divergent chromatin states would reduce the signal-to-noise ratio and would lead to
659 lower detection rates of DNA-DNA interactions. Significant changes in the transcriptome during
660 development are well documented in *S. macrospora* (3). Other studies have demonstrated a strong
661 connection between detectable changes of chromatin architecture and gene expression (75), so it can
662 be assumed that the transcriptional changes of *S. macrospora* during sexual development might be
663 accompanied by significant changes of DNA-DNA interaction frequency. A lower resolution of regularly
664 detectable interactions in the older wild type that is generating multiple cell types supports these
665 assumptions and might be another sign of chromatin state changes that accompany multicellular
666 development.
667 The Hi-C analysis of the ∆asf1 mutant revealed a large duplicated region on chromosome 2. We
668 hypothesized that the presence of this duplication might not be just a coincidence, but could be linked
669 to the surprising viability of the ∆asf1 mutant in *S. macrospora*. To the best of our knowledge, this
670 ascomycete is one of only two multicellular organisms that are known to survive loss of *asf1* (6, 17).
671 Genetic crosses confirmed co-segregation of the ∆asf1 allele on chromosome 6 with the duplication
672 on chromsome 2, whereas the wild type *asf1* allele and the duplication were able to recombine freely.
673 These findings support the hypothesis that the viability of the ∆asf1 mutant is coupled to the presence
674 of the duplication. Which specific role this region on chromosome 2 plays in the network of ASF1 is still
675 unclear. So far, no documented interaction partners or parts of the ASF1 network seem to be encoded
676 in this region. We assume that candidate genes in the duplication contribute to DNA damage repair or
677 protection, since during the crossing experiments we included *asf1* strains which express ASF1 variants
678 with specific amino acid substitutions, and one ASF1-V94R variant did not contain the duplication of
679 the area of interest. This variant is unable to perform the histone chaperone function of ASF1, due to
680 its inability to bind histones and is also unable to complement the development phenotype of *S.*
681 *macrospora* Δasf1. However, it is able to complement the sensitivity to genotoxic stress of ∆asf1. Thus,
682 a strain that is able to perform the DNA-damage protection function of ASF1 is not dependent on the

683 presence of the duplication on chromosome 2, therefore a role of the duplicated region in DNA-
684 damage protection might be conceivable.
685 Summarizing our work, we discovered that the ability of ASF1 to interact with histones is essential for
686 sexual development of *S. macrospora*, a function that also depends on the presence of large part of
687 the less conserved C-terminus of ASF1. Histone binding however, proved not to be necessary to allow
688 ASF1 to contribute to the genotoxic stress response. ChIP-seq experiments showed that ASF1 is
689 involved in the establishment of H3K56ac and the repression of H3K27me3. Furthermore, we
690 discovered a 600 kb duplication in the deletion mutant that appears to be linked to the surprising
691 viability of *S. macrospora* Δasf1. Future work might be able to shed light on how ASF1 regulates gene
692 expression by histone modification and which genes of the duplicated area are necessary to stabilize
693 *asf1* deletion mutants.
694
695
696 **Acknowledgements**
697 The authors would like to thank Silke Nimtz, Susanne Schlewinski and Tanja Rollnik for excellent
698 technical assistance and Christopher Grefen for support at the Department of Molecular and Cellular
699 Botany. The authors acknowledge the NGS team of the Omics CF NGS Unit (in development) and
700 CeBiTec. This work was funded by the German Research Foundation (DFG, grant NO407/7-2 to MN).
701
702
703 **References**
704 1. **Niklas KJ, Newman SA.** 2020. The many roads to and from multicellularity. Journal of
705 Experimental Botany **71:**3247-3253.
706 2. **Nagy LG, Kovács GM, Krizsán K.** 2018. Complex multicellularity in fungi: evolutionary
707 convergence, single origin, or both? Biol Rev **93:**1778-1794.
708 3. **Teichert I, Pöggeler S, Nowrousian M.** 2020. *Sordaria macrospora*: 25 years as a model
709 organism for studying the molecular mechanisms of fruiting body development. Appl
710 Microbiol Biotechnol **104:**3691-3704.
711 4. **Lord KM, Read ND.** 2011. Perithecium morphogenesis in *Sordaria macrospora*. Fungal Genet
712 Biol **48:**388-399.
713 5. **Nowrousian M.** 2018. Genomics and transcriptomics to study fruiting body development: An
714 update. Fungal Biology Reviews **32:**231-235.
715 6. **Gesing S, Schindler D, Fränzel B, Wolters D, Nowrousian M.** 2012. The histone chaperone
716 ASF1 is essential for sexual development in the filamentous fungus *Sordaria macrospora*. Mol
717 Microbiol **84:**748-765.
718 7. **English CM, Adkins MW, Carson JJ, Churchill ME, Tyler JK.** 2006. Structural basis for the
719 histone chaperone activity of ASF1. Cell **127:**495-508.
720 8. **Yamane K, Mizuguchi T, Cui B, Zofall M, Noma K, Grewal SI.** 2011. ASF1/HIRA facilitate global
721 histone deacetylation and associate with HP1 to promote nucleosome occupancy at
722 heterochromatic loci. Mol Cell **41:**56-66.
723 9. **Lercher L, Danilenko N, Kirkpatrick J, Carlomagno T.** 2018. Structural characterization of the
724 ASF1-RTT109 interaction and its role in histone acetylation. Nucleic Acids Res **46:**2279-2289.

725 10. **Clément C, Orsi GA, Gatto A, Boyarchuk E, Forest A, Hajj B, Miné-Hattab J, Garnier M, Gurard-**
726 **Levin ZA, Quivy J-P, Almouzni G.** 2018. High-resolution visualization of H3 variants during
727 replication reveals their controlled recycling. Nature Communications **9:**3181.
728 11. **Prado F, Cortés-Ledesma F, Aguilera A.** 2004. The absence of the yeast chromatin assembly
729 factor ASF1 increases genomic instability and sister chromatid exchange. EMBO Rep **5:**497-
730 502.
731 12. **Groth A, Ray-Gallet D, Quivy J-P, Lukas J, Bartek J, Almouzni G.** 2005. Human ASF1 Regulates
732 the Flow of S Phase Histones during Replicational Stress. Molecular Cell **17:**301-311.
733 13. **Tagami H, Ray-Gallet D, Almouzni G, Nakatani Y.** 2004. Histone H3.1 and H3.3 complexes
734 mediate nucleosome assembly pathways dependent or independent of DNA synthesis. Cell
735 **116:**51-61.
736 14. **Le S, Davis C, Konopka JB, Sternglanz R.** 1997. Two new S-phase-specific genes from
737 *Saccharomyces cerevisiae*. Yeast **13:**1029-1042.
738 15. **Singer MS, Kahana A, Wolf AJ, Meisinger LL, Peterson SE, Goggin C, Mahowald M, Gottschling**
739 **DE.** 1998. Identification of high-copy disruptors of telomeric silencing in *Saccharomyces*
740 *cerevisiae*. Genetics **150:**613-632.
741 16. **Tyler JK, Adams CR, Chen SR, Kobayashi R, Kamakaka RT, Kadonaga JT.** 1999. The RCAF
742 complex mediates chromatin assembly during DNA replication and repair. Nature **402:**555-
743 560.
744 17. **Zhu Y, Weng M, Yang Y, Zhang C, Li Z, Shen WH, Dong A.** 2011. *Arabidopsis* homologues of
745 the histone chaperone ASF1 are crucial for chromatin replication and cell proliferation in plant
746 development. Plant J **66:**443-455.
747 18. **Schumacher DI, Lütkenhaus R, Altegoer F, Teichert I, Kück U, Nowrousian M.** 2018. The
748 transcription factor PRO44 and the histone chaperone ASF1 regulate distinct aspects of
749 multicellular development in the filamentous fungus *Sordaria macrospora*. BMC Genetics
750 **19:**112.
751 19. **Mousson F, Lautrette A, Thuret JY, Agez M, Courbeyrette R, Amigues B, Becker E, Neumann**
752 **JM, Guerois R, Mann C, Ochsenbein F.** 2005. Structural basis for the interaction of ASF1 with
753 histone H3 and its functional implications. Proc Natl Acad Sci U S A **102:**5975-5980.
754 20. **Esser K.** Cryptogams : cyanobacteria, algae, fungi, lichens : textbook and practical guide, p. *In*
755 (ed),
756 21. **Walz M, Kück U.** 1995. Transformation of *Sordaria macrospora* to hygromycin B resistance:
757 characterization of transformants by electrophoretic karyotyping and tetrad analysis. Curr
758 Genet **29:**88-95.
759 22. **Kück U, Pöggeler S, Nowrousian M, Nolting N, Teichert I.** 2009. *Sordaria macrospora*, a Model
760 System for Fungal Development, p 17-39 doi:10.1007/978-3-642-00286-1_2.
761 23. **Oldenburg KR, Vo KT, Michaelis S, Paddon C.** 1997. Recombination-mediated PCR-directed
762 plasmid construction *in vivo* in yeast. Nucleic Acids Res **25:**451-452.
763 24. **Terfrüchte M, Joehnk B, Fajardo-Somera R, Braus GH, Riquelme M, Schipper K, Feldbrügge**
764 **M.** 2014. Establishing a versatile Golden Gate cloning system for genetic engineering in fungi.
765 Fungal Genet Biol **62:**1-10.
766 25. **Nowrousian M, Masloff S, Pöggeler S, Kück U.** 1999. Cell differentiation during sexual
767 development of the fungus *Sordaria macrospora* requires ATP citrate lyase activity. Mol Cell
768 Biol **19:**450-460.
769 26. **Bayram O, Krappmann S, Ni M, Bok JW, Helmstaedt K, Valerius O, Braus-Stromeyer S, Kwon**
770 **NJ, Keller NP, Yu JH, Braus GH.** 2008. VelB/VeA/LaeA complex coordinates light signal with
771 fungal development and secondary metabolism. Science **320:**1504-1506.
772 27. **Laemmli UK.** 1970. Cleavage of structural proteins during the assembly of the head of
773 bacteriophage T4. Nature **227:**680-685.
774 28. **Colot HV, Park G, Turner GE, Ringelberg C, Crew CM, Litvinkova L, Weiss RL, Borkovich KA,**
775 **Dunlap JC.** 2006. A high-throughput gene knockout procedure for Neurospora reveals
776 functions for multiple transcription factors. Proc Nat Acad Sci USA **103:**10352-10357.

29. **Engh I, Würtz C, Witzel-Schlömp K, Zhang Hai Y, Hoff B, Nowrousian M, Rottensteiner H, Kück U.** 2007. The WW Domain Protein PRO40 Is Required for Fungal Fertility and Associates with Woronin Bodies. Eukaryotic Cell **6:**831-843.
30. **Traeger S, Altegoer F, Freitag M, Gabaldon T, Kempken F, Kumar A, Marcet-Houben M, Pöggeler S, Stajich JE, Nowrousian M.** 2013. The genome and development-dependent transcriptomes of *Pyronema confluens*: a window into fungal evolution. PLoS Genet **9:**e1003820.
31. **Vaser R, Sović I, Nagarajan N, Šikić M.** 2017. Fast and accurate de novo genome assembly from long uncorrected reads. Genome Res **27:**737-746.
32. **Walker BJ, Abeel T, Shea T, Priest M, Abouelliel A, Sakthikumar S, Cuomo CA, Zeng Q, Wortman J, Young SK, Earl AM.** 2014. Pilon: an integrated tool for comprehensive microbial variant detection and genome assembly improvement. PLOS ONE **9:**e112963.
33. **Blank-Landeshammer B, Teichert I, Märker R, Nowrousian M, Kück U, Sickmann A.** 2019. Combination of proteogenomics with peptide *de novo* sequencing identifies new genes and hidden posttranscriptional modifications. mBio **10:**e02367-02319.
34. **Altschul SF, Madden TL, Schaffer AA, Zhang J, Zhang Z, Miller W, Lipman DJ.** 1997. Gapped BLAST and PSI-BLAST: a new generation of protein database search programs. Nucleic Acids Res **25:**3389-3402.
35. **Nowrousian M, Stajich JE, Chu M, Engh I, Espagne E, Halliday K, Kamerewerd J, Kempken F, Knab B, Kuo HC, Osiewacz HD, Pöggeler S, Read ND, Seiler S, Smith KM, Zickler D, Kück U, Freitag M.** 2010. *De novo* assembly of a 40 Mb eukaryotic genome from short sequence reads: *Sordaria macrospora*, a model organism for fungal morphogenesis. PLoS Genet **6:**e1000891.
36. **Sović I, Šikić M, Wilm A, Fenlon SN, Chen S, Nagarajan N.** 2016. Fast and sensitive mapping of nanopore sequencing reads with GraphMap. Nat Commun **7:**11307.
37. **Basenko EY, Pulman JA, Shanmugasundram A, Harb OS, Crouch K, Starns D, Warrenfeltz S, Aurrecoechea C, Stoeckert CJJ, Kissinger J, Roos DS, Hertz-Fowler C.** 2018. FungiDB: An integrated bioinformatic resource for fungi and oomycetes. J Fungi **4:**39.
38. **Galagan JE, Calvo SE, Borkovich KA, Selker EU, Read ND, Jaffe D, FitzHugh W, Ma LJ, Smirnov S, Purcell S, Rehman B, Elkins T, Engels R, Wang S, Nielsen CB, Butler J, Endrizzi M, Qui D, Ianakiev P, Bell-Pedersen D, Nelson MA, Werner-Washburne M, Selitrennikoff CP, Kinsey JA, Braun EL, Zelter A, Schulte U, Kothe GO, Jedd G, Mewes W, Staben C, Marcotte E, Greenberg D, Roy A, Foley K, Naylor J, Stange-Thomann N, Barrett R, Gnerre S, Kamal M, Kamvysselis M, Mauceli E, Bielke C, Rudd S, Frishman D, Krystofova S, Rasmussen C, Metzenberg RL, Perkins DD, Kroken S, et al.** 2003. The genome sequence of the filamentous fungus *Neurospora crassa*. Nature **422:**859-868.
39. **Kurtz S, Phillippy A, Delcher AL, Smoot M, Shumway M, Antonescu C, Salzberg SL.** 2004. Versatile and open software for comparing large genomes. Genome Biol **5:**R12.
40. **Cantarel BL, Korf I, Robb SMC, Parra G, Ross E, Moore B, Holt C, Sánchez Alvarado A, Yandell M.** 2008. MAKER: An easy-to-use annotation pipeline designed for emerging model organism genomes. Genome Res **18:**188-196.
41. **Lowe TM, Eddy SR.** 1997. tRNAscan-SE: a program for improved detection of transfer RNA genes in genomic sequence. Nucl Acids Res **25:**955-964.
42. **Carver T, Harris SR, Berriman M, Parkhill J, McQuillan JA.** 2012. Artemis: an integrated platform for visualization and analysis of high-throughput sequence-based experimental data. Bioinf **28:**464-469.
43. **Teichert I, Wolff G, Kück U, Nowrousian M.** 2012. Combining laser microdissection and RNA-seq to chart the transcriptional landscape of fungal development. BMC Genomics **13:**511.
44. **Kim D, Paggi JM, Park C, Bennett C, Salzberg SL.** 2019. Graph-based genome alignment and genotyping with HISAT2 and HISAT-genotype. Nat Biotech **37:**907-915.
45. **Bradford MM.** 1976. A rapid and sensitive method for the quantitation of microgram quantities of protein utilizing the principle of protein-dye binding. Analytical Biochemistry **72:**248-254.

46. **Huang X, Pan Q, Lin Y, Gu T, Li Y.** 2020. A native chromatin immunoprecipitation (ChIP) protocol for studying histone modifications in strawberry fruits. Plant Methods **16:**10.
47. **Chen S, Zhou Y, Chen Y, Gu J.** 2018. fastp: an ultra-fast all-in-one FASTQ preprocessor. Bioinformatics **34:**i884-i890.
48. **Li H, Durbin R.** 2010. Fast and accurate long-read alignment with Burrows–Wheeler transform. Bioinformatics **26:**589-595.
49. **Schulten A, Pietzenuk B, Quintana J, Scholle M, Feil R, Krause M, Romera-Branchat M, Wahl V, Severing E, Coupland G, Krämer U.** 2022. Energy status-promoted growth and development of Arabidopsis require copper deficiency response transcriptional regulator SPL7. Plant Cell **34:**3873-3898.
50. **Zhang Y, Liu T, Meyer CA, Eeckhoute J, Johnson DS, Bernstein BE, Nusbaum C, Myers RM, Brown M, Li W, Liu XS.** 2008. Model-based Analysis of ChIP-Seq (MACS). Genome Biology **9:**R137.
51. **Quinlan AR, Hall IM.** 2010. BEDTools: a flexible suite of utilities for comparing genomic features. Bioinformatics **26:**841-842.
52. **Heinz S, Benner C, Spann N, Bertolino E, Lin YC, Laslo P, Cheng JX, Murre C, Singh H, Glass CK.** 2010. Simple Combinations of Lineage-Determining Transcription Factors Prime cis-Regulatory Elements Required for Macrophage and B Cell Identities. Molecular Cell **38:**576-589.
53. **Open2C, Nezar A, Geoffrey F, Ilya MF, Aleksandra AG, Anton G, Maxim I, Sergey VV.** 2023. Pairtools: from sequencing data to chromosome contacts. bioRxiv doi:10.1101/2023.02.13.528389**:**2023.2002.2013.528389.
54. **Durand NC, Shamim MS, Machol I, Rao SS, Huntley MH, Lander ES, Aiden EL.** 2016. Juicer Provides a One-Click System for Analyzing Loop-Resolution Hi-C Experiments. Cell Syst **3:**95-98.
55. **Nowrousian M, Teichert I, Masloff S, Kück U.** 2012. Whole-genome sequencing of *Sordaria macrospora* mutants identifies developmental genes. G3 (Bethesda) **2:**261-270.
56. **Nowrousian M, Würtz C, Pöggeler S, Kück U.** 2004. Comparative sequence analysis of *Sordaria macrospora* and *Neurospora crassa* as a means to improve genome annotation. Fungal Genet Biol **41:**285-292.
57. **Malay AD, Umehara T, Matsubara-Malay K, Padmanabhan B, Yokoyama S.** 2008. Crystal structures of fission yeast histone chaperone Asf1 complexed with the Hip1 B-domain or the Cac2 C terminus. Journal of Biological Chemistry **283:**14022-14031.
58. **Daganzo SM, Erzberger JP, Lam WM, Skordalakes E, Zhang R, Franco AA, Brill SJ, Adams PD, Berger JM, Kaufman PD.** 2003. Structure and function of the conserved core of histone deposition protein ASF1. Curr Biol **13:**2148-2158.
59. **Dennehey BK, Noone S, Liu WH, Smith L, Churchill ME, Tyler JK.** 2013. The C terminus of the histone chaperone ASF1 cross-links to histone H3 in yeast and promotes interaction with histones H3 and H4. Mol Cell Biol **33:**605-621.
60. **Tamburini BA, Carson JJ, Linger JG, Tyler JK.** 2006. Dominant mutants of the *Saccharomyces cerevisiae* ASF1 histone chaperone bypass the need for CAF-1 in transcriptional silencing by altering histone and Sir protein recruitment. Genetics **173:**599-610.
61. **Tang M, Chen Z, Wang C, Feng X, Lee N, Huang M, Zhang H, Li S, Xiong Y, Chen J.** 2022. Histone chaperone ASF1 acts with RIF1 to promote DNA end joining in BRCA1-deficient cells. Journal of Biological Chemistry **298:**101979.
62. **Mao P, Wyrick JJ.** 2016. Emerging roles for histone modifications in DNA excision repair. FEMS Yeast Research **16:**fow090.
63. **Tsubota T, Berndsen CE, Erkmann JA, Smith CL, Yang L, Freitas MA, Denu JM, Kaufman PD.** 2007. Histone H3-K56 acetylation is catalyzed by histone chaperone-dependent complexes. Mol Cell **25:**703-712.
64. **Tsabar M, Waterman DP, Aguilar F, Katsnelson L, Eapen VV, Memisoglu G, Haber JE.** 2016. ASF1 facilitates dephosphorylation of RAD53 after DNA double-strand break repair. Genes Dev **30:**1211-1224.

881 65. **Bannister AJ, Kouzarides T.** 2011. Regulation of chromatin by histone modifications. Cell Res
882 **21:**381-395.
883 66. **Boros J, Arnoult N, Stroobant V, Collet JF, Decottignies A.** 2014. Polycomb repressive complex
884 2 and H3K27me3 cooperate with H3K9 methylation to maintain heterochromatin protein 1α
885 at chromatin. Mol Cell Biol **34:**3662-3674.
886 67. **Hugues A, Jacobs CS, Roudier F.** 2020. Mitotic Inheritance of PRC2-Mediated Silencing:
887 Mechanistic Insights and Developmental Perspectives. Frontiers in Plant Science **11**.
888 68. **Basenko EY, Sasaki T, Ji L, Prybol CJ, Burckhardt RM, Schmitz RJ, Lewis ZA.** 2015. Genome-
889 wide redistribution of H3K27me3 is linked to genotoxic stress and defective growth. Proc Natl
890 Acad Sci U S A **112:**E6339-6348.
891 69. **Hagarman JA, Motley MP, Kristjansdottir K, Soloway PD.** 2013. Coordinate regulation of DNA
892 methylation and H3K27me3 in mouse embryonic stem cells. PLoS One **8:**e53880.
893 70. **Lee CY, Grant PA.** 2019. Chapter 1-1 - Role of Histone Acetylation and Acetyltransferases in
894 Gene Regulation, p 3-30. *In* McCullough SD, Dolinoy DC (ed), Toxicoepigenetics
895 doi:https://doi.org/10.1016/B978-0-12-812433-8.00001-0. Academic Press.
896 71. **Driscoll R, Hudson A, Jackson SP.** 2007. Yeast RTT109 promotes genome stability by
897 acetylating histone H3 on lysine 56. Science **315:**649-652.
898 72. **Adkins MW, Carson JJ, English CM, Ramey CJ, Tyler JK.** 2007. The Histone Chaperone Anti-
899 silencing Function 1 Stimulates the Acetylation of Newly Synthesized Histone H3 in S-phase*.
900 Journal of Biological Chemistry **282:**1334-1340.
901 73. **Wurtele H, Kaiser GS, Bacal J, St-Hilaire E, Lee EH, Tsao S, Dorn J, Maddox P, Lisby M, Pasero**
902 **P, Verreault A.** 2012. Histone H3 lysine 56 acetylation and the response to DNA replication
903 fork damage. Mol Cell Biol **32:**154-172.
904 74. **Banigan EJ, Tang W, van den Berg AA, Stocsits RR, Wutz G, Brandão HB, Busslinger GA, Peters**
905 **J-M, Mirny LA.** 2023. Transcription shapes 3D chromatin organization by interacting with loop
906 extrusion. Proceedings of the National Academy of Sciences **120:**e2210480120.
907 75. **Almassalha LM, Tiwari A, Ruhoff PT, Stypula-Cyrus Y, Cherkezyan L, Matsuda H, Dela Cruz**
908 **MA, Chandler JE, White C, Maneval C, Subramanian H, Szleifer I, Roy HK, Backman V.** 2017.
909 The Global Relationship between Chromatin Physical Topology, Fractal Structure, and Gene
910 Expression. Sci Rep **7:**41061.

911

912

913

914

915

916

917

918

919

920 **Tables**

921
922
923
924 **Table 1.** Transformants and fertility rates for complementation experiments of ∆asf1 with ASF1
925 variants.

Encoded ASF1 variant	No. of primary transformants	Fertile transformants	Sterile transformants	Percantage of fertile transformants
Wild type	53	47	6	88.7
D37A	61	41	20	67.2
V94R	41	0	41	0
152T	19	0	19	0
185T	22	0	22	0
210T	18	15	3	83.3

926
927
928
929 **Table 2.** Presence of the duplication on chromosome 2 in wild type and *asf1* deletion strains. Strains
930 were obtained from crosses of ∆asf1 with the spore color mutant fus, which carries the wild type *asf1*
931 gene. The full list of tested strains has been added as Supplemental table 5.

Genotype	No. of tested strains	No. of strains with duplication	Percentage of strains with duplication
Wild type	69	21	30.4
Δasf1	37	37	100

932
933
934

Figures

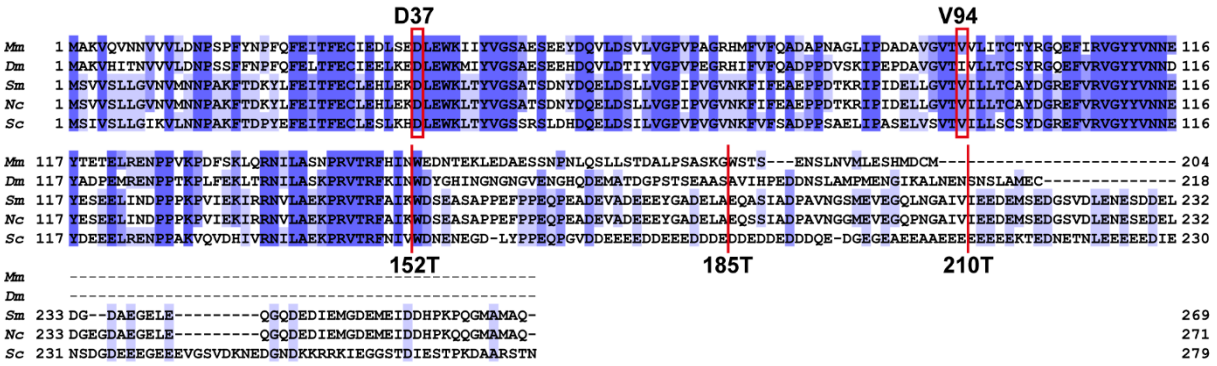

Figure 1. Alignment of ASF1 amino acid sequences of several animal and fungal model organisms. The first 152 amino acids are highly conserved. The C-terminal region is more divergent and parts of it exist only in fungi. Positions D37 and V94 were substituted for functional analysis in this study. D37 is known as a HIRA interaction site in *Schizosaccharomyces pombe* (57), while V94 has been established as the H3-H4 interaction site (7, 19). Positions 152, 185 and 210 were targeted to create truncated ASF1 variants. Abbreviations and accession numbers: *Mm*, *Mus musculus* (AAH27628.1); *Dm*, *Drosophila melanogaster* (NP_524163.1); *Sm*, *Sordaria macrospora* (KAA8632619.1); *Nc*, *Neurospora crassa* (XP_958588.1); *Sc*, *Saccharomyces cerevisiae* (NP_012420.1).

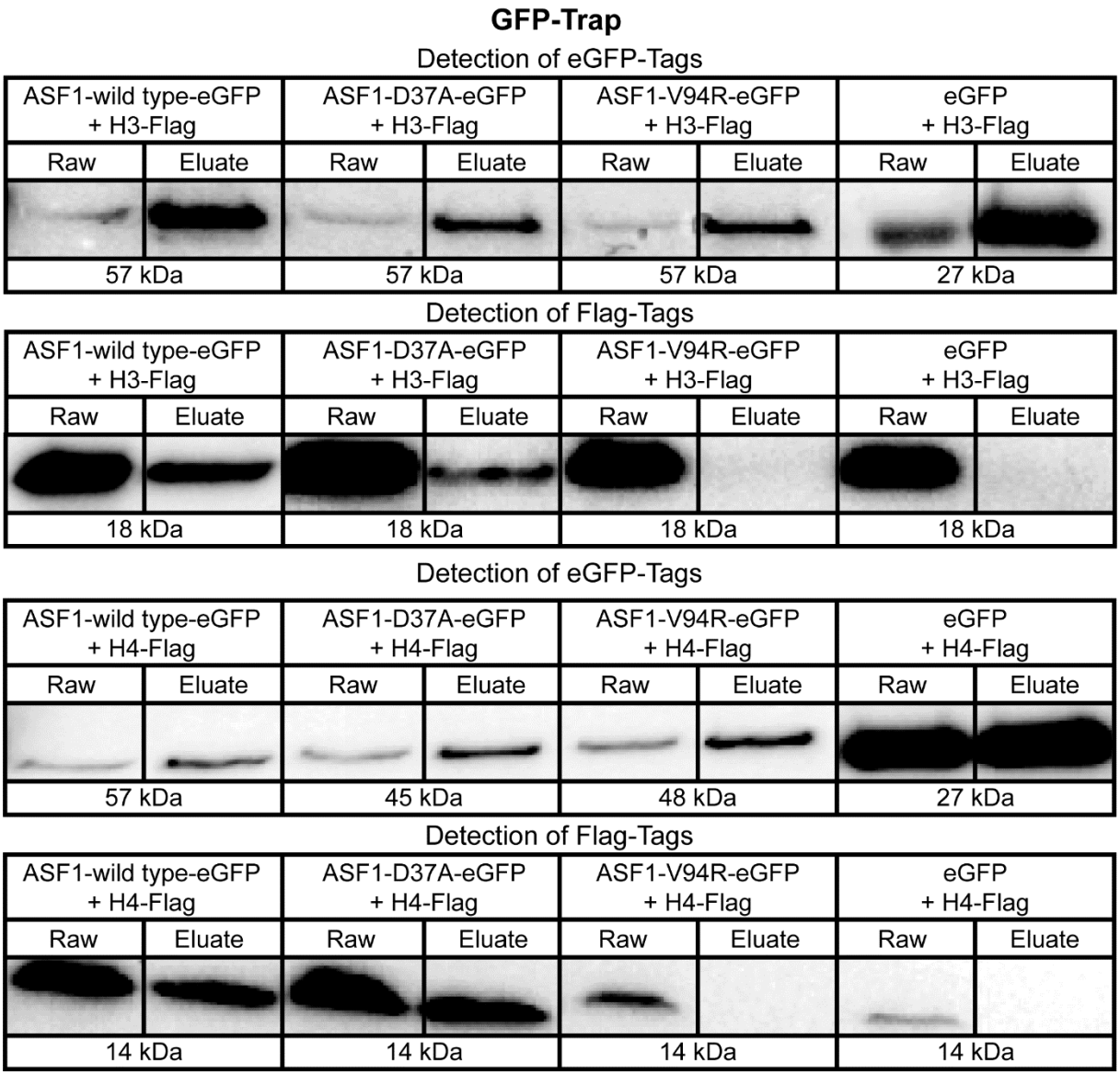

Figure 2. Co-immunoprecipitation results for ASF1 variants with amino acid substitutions. GFP-tagged ASF1 wild type and variants D37A and V94R were used as bait proteins for Flag-tagged histones H3 and H4 in a GFP trap. Results were checked by western blot analysis with antibodies against GFP and Flag tags. ASF1 wild type and the D37A variant showed signals for bait and prey proteins in the raw and eluate sample, indicating interaction, whereas the V94R variant showed the signal for the prey protein only in the raw sample. Strains expressing non-fused eGFP with the corresponding Flag-tagged histones were used as a negative control. The corresponding results with histones H3 and H4 as baits are shown in Supplemental Figure 2.

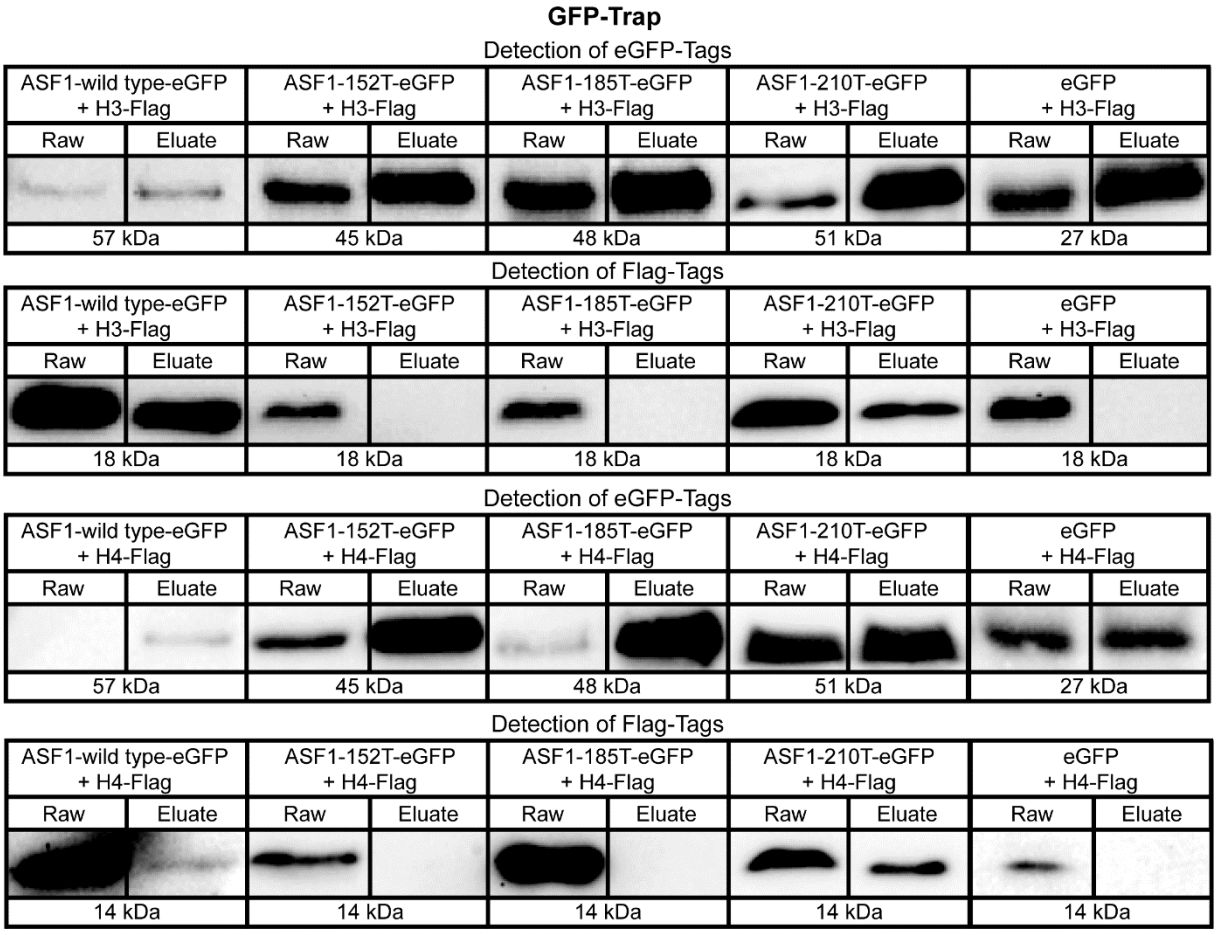

Figure 3. Co-immunoprecipitation results for truncated ASF1 variants. GFP-tagged ASF1 wild type and variants 152T, 185T and 210T were used as bait proteins for Flag-tagged histones H3 and H4 in a GFP trap. Results were checked by western blot analysis with antibodies against GFP and Flag tags. ASF1 wild type and the 210T variant showed signals for bait and prey proteins in the raw and eluate sample, indicating interaction, whereas the 152T and 185T variants showed the signal for the prey protein only in the raw sample. Strains expressing non-fused eGFP with the corresponding Flag-tagged histones were used as a negative control. The corresponding results with histones H3 and H4 as baits are shown in Supplemental Figure 3.

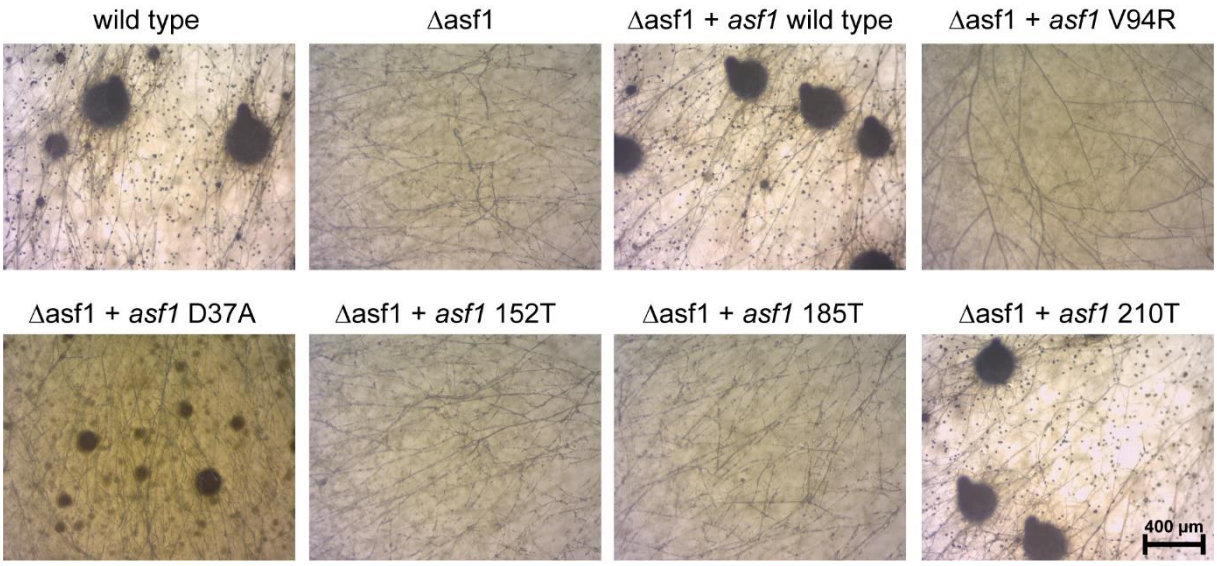

Figure 4. Phenotypes of strains from Δasf1 complementation experiments. The wild type generates mature perithecia in 7 days, while the development of the deletion mutant is blocked at the stage of early protoperithecia and mostly generates only vegetative mycelium. Reintroducing the *asf1* wild type gene into the deletion mutant fully complements the phenotype and lead to strains that are indistinguishable from the wild type. Transforming Δasf1 with the *asf1* V94R variant did not complement the mutant strain resulting in strains with the sterile phenotype of Δasf1. A D37A variant partially complements the mutant, such strains are fertile, but show distinct developmental aberrations like a tendency to generate mostly large protoperithecia and a brown coloration of the mycelium. Transformation with truncated *asf1* variants did not lead to complementation with variants 152T and 185T, but the longer 210T variant led to strains that show a wild type phenotype again.

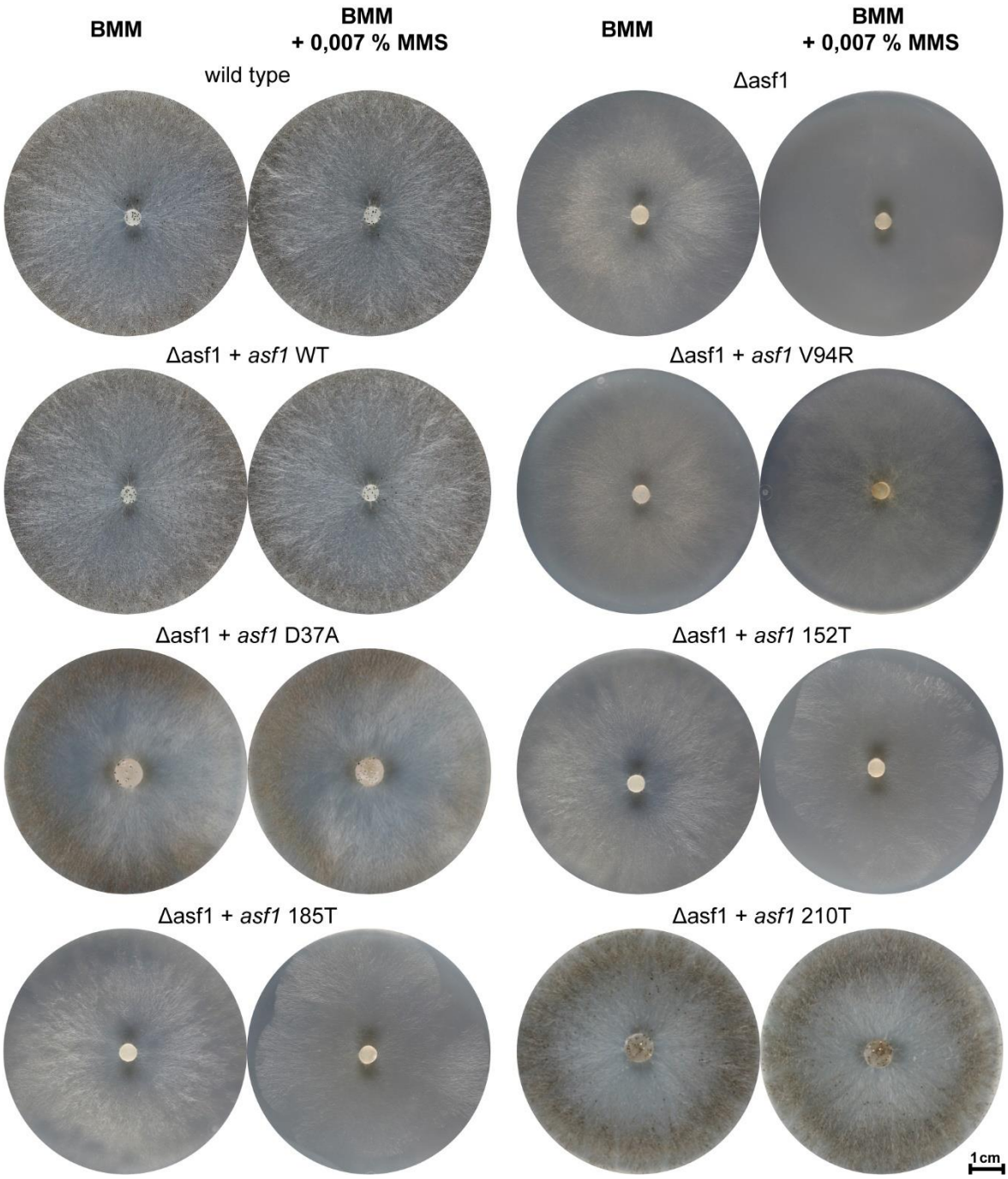

Figure 5. Genotoxic stress resistance of *S. macrospora* strains expressing ASF1 variants. At the given MMS concentration, the wild type was able to grow normally, while the *asf1* deletion mutant exhibited severe sensitivity (no growth). Reintroducing the wild type *asf1* into the mutant restored the resistance. All strains that expressed any kind of ASF1 variant showed at least partial resistance to genotoxic stress, even variants that were shown to be unable to interact with histones and do not complement the developmental defects of *S. macrospora* Δasf1.

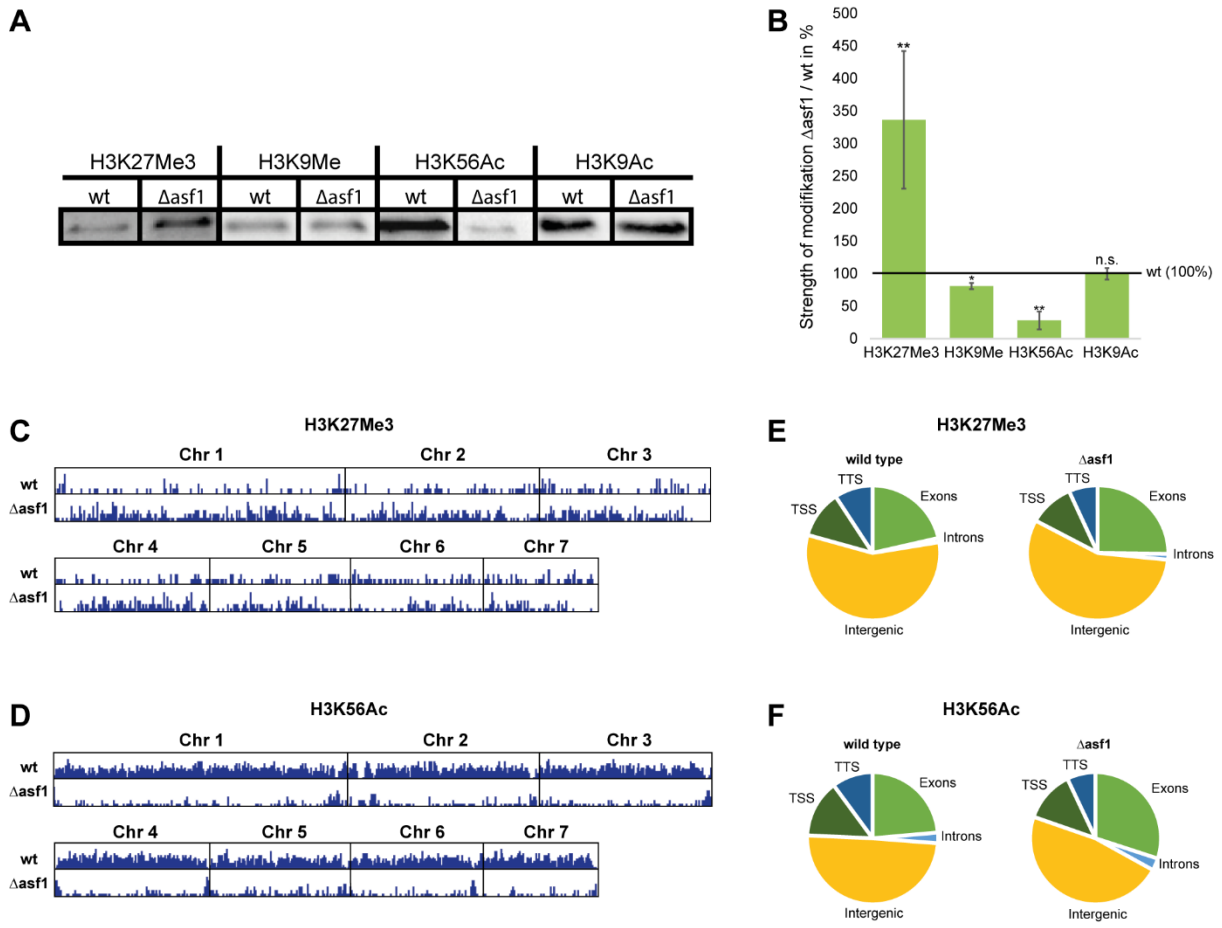

Figure 6. Analysis of histone modifications in the wild type and Δasf1.

A. Semiquantitative screening for histone modifications affected by ASF1. Western blots with antibodies against the indicated histone modifications were used to compare the band strength of equal amounts of protein from wild type and Δasf1 extracts.

B. The band intensity in Western Blots was measured densiometrically in 5 independent biological replicates and the ratio of Δasf1 versus wild type was calculated. The deletion mutant showed a significant increase in H3K27me3 and significant decreases in H3K9me and H3K56ac, while H3K9ac was not affected by an *asf1* deletion. Student's t-test for significance: * = p-value < 0.05; ** = p-value < 0.01.

C and D. Uniquely H3K27 trimethylated positions (C) and uniquely H3K56 acetylated positions (D) across the *S. macrospora* genome in wild type and Δasf1. ChiP-Seq revealed a general increase in H3K27me3 and decrease in H3K56ac across the genome in Δasf1 compared to the wild type. 401 unique positions carried H3K27me3 in the wild type, while this mark was present at 1142 unique positions in the mutant. For H3K56ac, 4736 unique positions were found for H3K56ac in the wild type and 664 unique positions in the mutant (Supplemental table 6).

E and F. Relative distribution of H3K27me3 (E) and H3K56ac (F) in annotated regions of *S. macrospora* in wild type and Δasf1. Although the general amount of H3K27me3 was increased in the deletion mutant, we did not observe a significant change in the relative positioning of this mark across the shown genomic regions aside from a slight shift from intergenic to exonic regions. An *asf1* deletion leads to a significant decrease of unique H3K56ac positions compared to the wild type, but it appears that a relative increase can be observed in exonic regions.

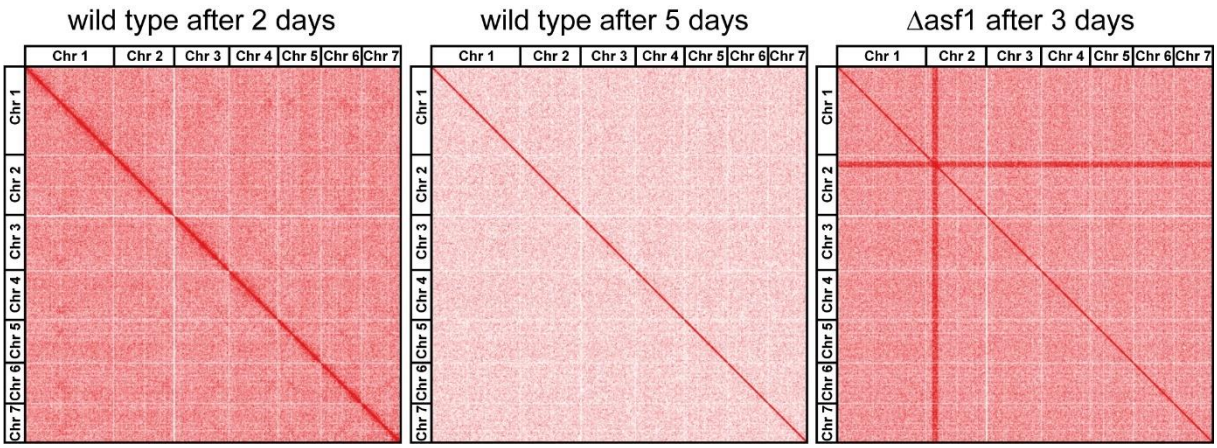

Figure 7. Hi-C analysis of *S. macrospora* wild type and Δasf1. DNA-DNA interactions recorded in the samples at the given time were plotted against both interacting positions in the genome. Each red dot represents an interaction event. The characteristic red diagonal indicates highly increased interaction frequencies of adjacent positions that are always in close proximity to each other. Even in the younger, mostly vegetative state, the resolution was not high enough to make out specific compartments of the genome, even though some areas of heightened interaction frequencies can be observed. The resolution was much lower in the older sample that has progressed further in the developmental cycle. This might be an indicator of different chromatin states that could be present in cells that are only generated during sexual development. Strong horizontal and vertical lines were detectable in the deletion mutant that appeared to indicate higher interaction frequencies originating from a 600 kb are on chromosome 2 and were subsequently shown to be caused by a duplication of a region on chromosome 2.

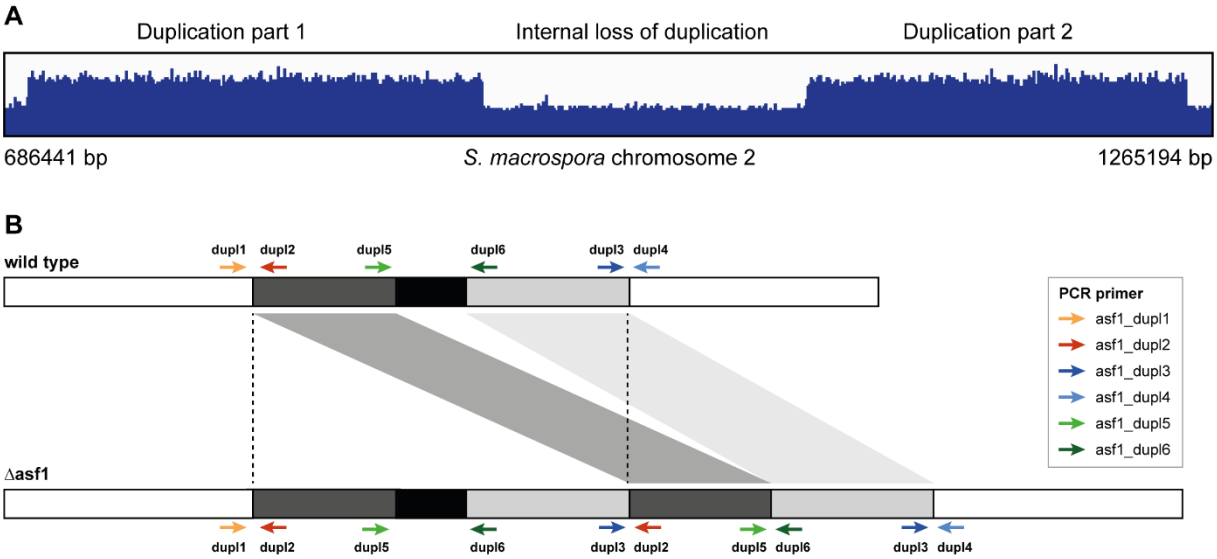

Figure 8. Confirmation of a duplication on chromosome 2 in the *asf1* deletion mutant by genome sequencing.

A. Whole genome sequencing of *S. macrospora* Δasf1 confirmed the presence of a duplication in a region of around 600 kb on chromosome 2. The alignment of the reads from sequencing of the mutant genome to the wild type reference genome shows that the duplication consists of two parts, indicating either two separate duplication events or the loss of the internal area of the duplicated region.

B. Schematics for a putative duplication on chromosome 2 of *S. macrospora* Δasf1. Whole genome sequencing proved the presence of a duplication. To test our hypothesis of a tandem duplication with an internal loss event, PCR tests with primers amplifying the genomic borders in the wild type or the newly created, duplication-specific junctions were designed. While the wild type should only yield PCR products for the external borders of the area of interest (asf1_dupl1 x asf1_dupl2, asf1_dupl3 x asf1_dupl4), strains possessing a tandem duplication should also generate products for the new junctions of the duplicated area (asf1_dupl3 x asf1_dupl2) and of the internal region lost in the duplication (asf1_dupl5 x asf1_dupl6).